AN ABSTRACT OF THE THESIS OF

Kevin C. Kemper for the degree of Master of Science in Mechanical Engineering presented on March 19, 2012.

Title:

Passive Dynamics and Their Influence on Performance of Physical Interaction Tasks

Abstract approved: ______________________________________

Jonathan W. Hurst

For robotic manipulation tasks in uncertain environments, research typically revolves around developing the best possible software control strategy. However, the passive dynamics of the mechanical system, including inertia, stiffness, damping and torque limits, often impose performance limitations that cannot be overcome with software control. Discussions about the passive dynamics are often imprecise, lacking comprehensive details about the physical limitations. In the first half of this paper, we develop relationships between an actuator's passive dynamics and the resulting performance, to better understanding how to tune the passive dynamics. We characterize constant-contact physical interaction tasks into two different tasks that can be roughly approximated as force control and position control and calculate the required input to produce a desired output. These exact solutions provide a basis for understanding how the parameters of the mechanical system affect the overall system's bandwidth limit without limitations of a specific control

algorithm. We then present our experimental results compared to the analytical prediction for each task using a bench top actuator. Our analytical and experimental results show what, until now, has only been intuitively understood: soft systems are better at force control, stiff systems are better at position control, and there is no way to optimize an actuator for both tasks.

Passive Dynamics and Their Influence on Performance of Physical Interaction Tasks

by

Kevin C. Kemper

A THESIS

submitted to

Oregon State University

in partial fulfillment of
the requirements for the
degree of

Master of Science

Presented March 19, 2012
Commencement June 2012

Master of Science thesis of Kevin C. Kemper presented on March 19, 2012.

APPROVED:

Major Professor, representing Mechanical Engineering

Head of the School of Mechanical Industrial and Manufacturing Engineering

Dean of the Graduate School

I understand that my thesis will become part of the permanent collection of Oregon State University libraries. My signature below authorizes release of my thesis to any reader upon request.

Kevin C. Kemper, Author

ACKNOWLEDGMENTS

I would like to thank my colleagues in the Dynamic Robotics Laboratory for their collaboration and friendship. I would also like to thank all of the people in the Electrical Engineering and Computer Science department - in particular Donald Heer and the Tekbots program - for giving me the freedom help to push myself technically while an undergraduate at OSU.

I would like to especially thank my major adviser, Jonathan W. Hurst, for all of his guidance and support. Without his help, I would have never found the opportunities to excel that I enjoy today.

Funding for this work was provided by the Defense Advanced Research Projects Agency and the National Science Foundation.

TABLE OF CONTENTS

TABLE OF CONTENTS (Continued)

LIST OF FIGURES

LIST OF FIGURES (Continued)

LIST OF FIGURES (Continued)

LIST OF FIGURES (Continued)

LIST OF TABLES

Chapter 1 – Introduction

Humans are able to achieve a wide range of physical interaction tasks, including freehand machining of wood and riding in a car without spilling a cup of coffee, because they actively change the passive dynamic properties of their arm through co-contraction of antagonistic muscles. When using a router to machine wood, the woodworker's muscles are tensed, and his arm is as rigid and stiff as he can make it; and even so, the performance is much lower than a much more rigid CNC machine. In contrast, when stabilizing a cup of coffee, the passenger's arm largely relaxes reducing the arm stiffness; even so, the performance is much lower than a much less stiff Steadicam camera stabilization rig.

Robots excel at precise position control and are useful for tasks that make use of this ability, such as CNC machining. However, physical interaction tasks such as catching a ball, walking, running, grasping unknown objects, constrained contact and even simple force or torque control have historically been difficult for robots. Each of these tasks involve dynamic effects such as unexpected impacts and/or a significant transfer of kinetic energy between the robot and its environment. Animals far outperform robots at many of these tasks, and we contend that this is due to inherent mechanical limitations in traditional robotic mechanisms rather than software control inadequacies. This paper focuses on how an actuator's passive dynamics affect its bandwidth performance in continuous-contact physical interaction.

Consider a traditional industrial robot arm, powered by electric motors with large gear reductions and rigid links. The traditional approach to force control utilizes such an arm, with a force sensor placed at the end-effector. Forces are measured, software controllers calculate the desired motor torques and the motors move accordingly. However, the motors have inertia, which is amplified through the gearbox into a significant reflected inertia, and combines with torque limitations on the motors to limit their acceleration. These passive dynamics cannot be overcome using software control. If an object impacts the arm, such as a baseball, the motors will have no chance to respond, the arm will behave as a rigid inertial object and the software control will have no part in its initial dynamic response.

Researchers at the Massachusetts Institute of Technology (MIT) Leg Laboratory explored these ideas and created an actuator designed specifically to include an elastic element as a force sensor and low impedance coupling between the drive system and the load to improve force control. The system is aptly dubbed a series elastic actuator (MIT-SEA) and it has been shown that this configuration provides filtering to handle shock loads as well as higher bandwidth force control [1, 2]. MIT-SEAs offer great advantages, however, there are only approximate guidelines for how a specific stiffness changes the performance of the actuator. To understand how the mechanical elements of an actuator specifically modifies - for better or worse - its performance, we extend the base MIT-SEA to include damping as well as realistic physical limitations such as motor torque limits and inertia.

The work in this thesis lays out a mathematical framework for characterizing a mechanical system that includes a motor with inertia and torque limits, a series

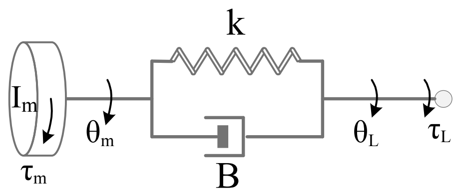

Figure 1.1: The base system investigated in this research. The model includes damping, elasticity, motor inertia and torque limits. The actuator is constrained such that only θ_m and θ_L can move.

spring and a series damper, as shown in Fig. 1.1. We investigate three examples of interaction tasks; applying constant force to a moving object, applying changing force to a stationary object and catching/stopping an unknown object without allowing it to bounce. We then describe the mathematically optimal passive dynamics required to achieve the best possible bandwidth, based on fundamental physical limits. A summary of the contributions of this work:

- Developed a mathematical framework for characterizing a basic actuator mechanism.
  - Show how system parameters (such as motor inertia and transmission stiffness) affect performance.
- Analysis of three distinct tasks to describe performance boundaries:
  - Changing torque against a static surface.
  - Zero torque against a moving load.
  - Catching a mass without bouncing.

- Experimental results confirming that the mathematical model and predictions for changing torque against a static surface and zero torque against a moving load are valid.

In Chapter 2, we analytically show that a very compliant system is ideal for applying constant forces to moving objects (roughly analogous to force control), and a very stiff system is ideal for applying changing forces to a stationary object (roughly analogous to position control). Chapter 3 defines how an actuator's passive dynamics affect performance when experiencing an unexpected impact such as catching an object. Chapter 4 section of this paper experimentally validates the theory discussed in Chapter 2.

Based on this work, roboticists will be able to estimate that a mechanical system has the bandwidth necessary for a particular task, especially tasks involving force or torque control, spring-like behavior, impacts and kinetic energy transfer.

Chapter 2 – Optimal passive dynamics for torque/force control

For robotic manipulation tasks in uncertain environments, good force control can provide significant benefits. The design of force or torque controlled actuators typically revolves around developing the best possible software control strategy. However, the passive dynamics of the mechanical system, including inertia, stiffness, damping and torque limits, often impose performance limitations that cannot be overcome with software control. Discussions about the passive dynamics are often imprecise, lacking comprehensive details about the physical limitations. In this paper, we develop relationships between an actuator's passive dynamics and the resulting performance, for the purpose of better understanding how to tune the passive dynamics for a force control task. We present two distinct scenarios for the actuator system and calculate the required input to produce a desired output. These exact solutions provide a basis for understanding how the parameters of the mechanical system affect the overall system's bandwidth limit. Our model does not include active control; we computed the optimal input to the system to produce the required torque at the load with zero error. This is important so that our results only reflect the physical system's performance.

2.1 Introduction

Robots excel at precise position control and are useful for tasks that make use of this ability, such as CNC machining. However, physical interaction tasks such as catching a ball, walking, running, grasping unknown objects, constrained contact and even simple force or torque control have historically been difficult for robots. Each of these tasks involve dynamic effects such as unexpected impacts and/or a significant transfer of kinetic energy between the robot and its environment. Animals far outperform robots at many of these tasks, and we contend that this is due to inherent mechanical limitations in traditional robotic mechanisms rather than software control inadequacies. This paper focuses on how an actuator's passive dynamics affect force or torque control.

Consider a traditional industrial robot arm, powered by electric motors with large gear reductions and rigid links. The traditional approach to force control utilizes such an arm, with a force sensor placed at the end-effector. Forces are measured, software controllers calculate the desired motor torques and the motors move accordingly. However, the motors have inertia, which is amplified through the gearbox into a significant reflected inertia, and combines with torque limitations on the motors to limit their acceleration. These passive dynamics cannot be overcome using software control. If an object impacts the arm, such as a baseball, the motors will have no chance to respond, the arm will behave as a rigid inertial object and the software control will have no part in its dynamic response.

Passive dynamics are not always harmful. As an example of passive dynamics improving performance, a mechanical spring in series with a motor can dramatically

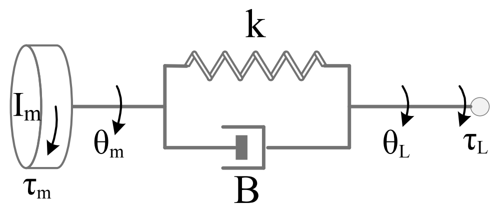

Figure 2.1: The system we investigate in this paper is entirely rotational and includes damping, elasticity, motor inertia and torque limits. The actuator is constrained such that only θ_m and θ_L can move.

improve force control bandwidth in response to position disturbances. However, this improvement applies only to the specific case of force control and its robustness to position disturbances; a series spring will reduce the performance of the system for position control. For peak performance in a robotic system, the passive dynamics must be tailored to the specific task. This is roughly analogous to impedance matching in electrical systems.

In this paper, we lay out a mathematical framework for mechanical systems that includes a motor with inertia and torque limits, a series spring and a series damper, as shown in Fig. 4.1. We investigate two examples; applying constant force to a moving object and applying changing force to a stationary object. We then describe the mathematically optimal passive dynamics required to achieve the best possible bandwidth, based on fundamental physical limits. Based on this work, roboticists will be able to estimate that a mechanical system has the bandwidth necessary for a particular task, especially tasks involving force or torque control, spring-like behavior, impacts and kinetic energy transfer.

2.2 Background

Muscular systems in animals incorporate elastic elements, which are most often examined while investigating locomotion, and are generally discussed in the context of energy storage [3][4] [5][6]. Roboticists have built machines designed to mimic this spring-like behavior [7] [8]. Although the designers of these running machines acknowledge that elasticity provides robustness, their studies generally focus on energy storage and efficiency, with little attention to force control.

Early investigations into force control found that series compliance in an actuator can increase stability, and in some cases is required for stable operation [9][10]. Researchers at the Massachusetts Institute of Technology (MIT) Leg Laboratory explored these ideas and created an actuator designed specifically to include an elastic element as a force sensor and low impedance coupling between the drive system and the load to improve force control. The system is aptly dubbed a series elastic actuator (MIT-SEA) and it has been shown that this configuration provides filtering to handle shock loads as well as higher resolution/bandwidth force control [1][2]. MIT-SEAs offer great advantages, however, there are only approximate guidelines for choosing an appropriate spring. Further work to improve the MIT-SEA has focused on control architecture [11][12] or transmission design [13][14].

Chew et al. proposed a similar actuator design using a viscous damper in place of the elastic element, dubbed a series damper actuator (SDA) [15]. They hypothesize that using damping, rather than elasticity, allows for greater bandwidth, and can be easily constructed to allow a variable damping coefficient. They admit that the main disadvantage of the SDA is the energy dissipation property, which limits the energy efficiency of the design. The developers of the SDA do not provide concrete relationships between damping and bandwidth, but present a conjecture relating the two.

A hybrid of the SDA and MIT-SEA has been proposed by Hurst et al. [16]. They concluded that the added damping provides higher bandwidth than a purely series-elastic element and reduces unwanted oscillations in specific situations. Initial force spikes observed by the drive system at impact are greater than would be observed by just an elastic element, but are still much less than for a perfectly stiff system.

2.3 System model

In this paper, we define relationships between series stiffness, series damping, drive system inertia and the drive system torque limits in specific experimental scenarios. To simplify the discussion, we use "motor" to describe the drive system as a whole - transmission and motor characteristics. The following symbols describe our model:

ω	Angular frequency	$\frac{rad}{s}$
k	Spring constant	$\frac{N \cdot m}{rad}$
B	Damping constant	$\frac{kg \cdot m^2}{s \cdot rad}$
I_m	Motor inertia	$kg \cdot m^2$
τ_m	Motor torque	$N \cdot m$
τ_{limit}	Motor torque limit	$N \cdot m$
τ_L	Load torque	$N \cdot m$
θ_m	Motor angle	rad
θ_L	Load angle	rad
θ_A	Load angle amplitude	rad

Our goal in this paper is to calculate the fundamental limitations of the physical system. Our model does not include active control; we compute the optimal input to the system to produce a desired torque at the load. This is an important distinction from previous attempts to develop actuators of this nature. By eliminating controller error, we are able isolate the physical limitations of our model.

To develop the relationships between an actuator's design parameters, we investigate the series elastic/damping actuator (SEDA) in Fig. 4.1. Our actuator includes damping and elasticity because they are both physically unavoidable and possibly useful. We want to know how to select these elements (k, B and I_m) to design the best possible actuator around a force or torque control task.

Our system model is entirely rotational because our lab, the Dynamic Robotics

Laboratory, is interested in developing robots that use electric motors. However, the concepts in this paper relate directly to force control as well as to torque control. Roboticists designing actuators with linear drive systems (such as hydraulic pistons) can use the relationships presented in this paper to develop linear systems.

In addition to the reactive elements k and B, we include motor torque limits as well as motor inertia. The torque limit and motor inertia are important for the calculation of the bandwidth. If infinite torque were possible, there would be no requirements for designing the impedance of the actuator. In other words, it would not matter how soft, or stiff, the elements were, just as long as they existed.

In the case of zero motor inertia with motor torque limits, the elastic and damping elements are no longer important. The elements just need to exist to provide for transmission of torque. In this case the largest torque the actuator could produce at the load would be the torque limit. In either case the system is optimal, has infinite bandwidth for any task and the impedance of the actuator is irrelevant. Unfortunately, this is not the case with real systems because all motors have torque limits and rotor inertia.

2.4 Actuation scenarios

Each scenario is designed to show that there is an optimal relationship between k, B and I_m for a distinct task. This paper focuses on simple, fundamental motions that might be expected from a force or torque controlled actuator. The goal is to relate k, B, I_m and τ_{limit} to the performance of a robotic actuator under specific conditions.

To determine the effect of k, B and I_m on the performance of the system in any test scenario, we first solve for the motor torque, τ_m, that produces the desired load torque, τ_L. If τ_m remains below the motor's peak torque limit, the system is able to achieve the desired performance goals.

In most cases, as the frequency of a task increases, the required motor torque increases and eventually meets the motor torque limit. The function for the exact motor torque, evaluated with torque limits, becomes the basis for describing the relationships that parameters have on achieving the maximum frequency of each task.

To find the required motor torque, we start by defining the differential equations that describe the motion of the system:

$$I_m\ddot{\theta}_m = \tau_m - \tau_B - \tau_k \tag{2.1}$$

$$0 = \tau_B + \tau_k - \tau_L \tag{2.2}$$

where:

$$\begin{aligned}\tau_k &= k[\theta_m - \theta_L] \\ \tau_B &= B[\dot{\theta}_m - \dot{\theta}_L].\end{aligned}$$

We then take the Laplace transform of (4.1) and (4.2), and solve for the s-domain equation of the motor torque ($T_m(s)$). With initial conditions ignored, this is calculated as:

$$T_m(s) = \Theta_L(s)\left(I_m s^2\right) + T_L(s)\left(\frac{I_m s^2 + Bs + k}{Bs + k}\right). \tag{2.3}$$

Equation (4.5) describes how the load motion and desired load torque affect the required motor torque, where $\Theta_L(s)$ is the s-domain representation of the load motion and $T_L(s)$ is the s-domain representation of the load torque. With this equation, we can define any motion for the load and a desired load torque and determine the exact requirement for the motor torque. At steady state, this computed motor torque will produce the torque at the load with zero error.

2.5 Changing torque against a static surface

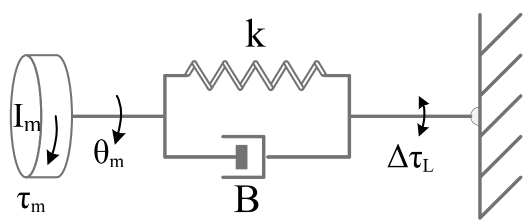

Figure 2.2: For the first scenario, the load is fixed to ground ($\theta_L = 0$) while the motor attempts to produce the desired τ_L through the passive dynamic elements k and B.

For the first task, our model applies a sinusoidal torque to a fixed load (Fig. 4.2). We demonstrate how k, B and I_m affect the maximum frequency at which the actuator can vary the applied torque. The maximum frequency for this case is defined as the frequency that the actuator can oscillate the torque at the load before steady-state error is encountered.

To evaluate the maximum frequency the actuator can achieve under a given set of values for k, B and I_m, we consider the point where the motor's torque becomes greater than the torque limit. At this point the motor is no longer able to produce the required torque to exactly generate the desired τ_L.

To find the motor torque as a function of time, $\tau_m(t)$, we define the motion of the load, $\theta_L(t)$ and the desired load torque, $\tau_L(t)$. For this scenario, we hold the load position constant (Fig. 4.2). We then define the desired load torque to be a sinusoidal function with some angular frequency, ω, and a fixed amplitude of 1 $N \cdot m$. Note that the amplitude can be greater or smaller without affecting the relationships as long as it is less than the torque limit:

$$\begin{aligned} \theta_L(t) &= 0 \\ \tau_L(t) &= sin(\omega t). \end{aligned} \tag{2.4}$$

Taking the Laplace transform of $\tau_L(t)$ gives:

$$T_L(s) = \frac{\omega}{s^2 + \omega^2}. \tag{2.5}$$

Plugging equation (4.8) back into (4.5) and taking the inverse Laplace transform, we find the $\tau_m(t)$ required to produce the $\tau_L(t)$ defined in (4.7) at steady state

$(t \gg 0)$:

$$\tau_m(t) = \left(\frac{I_m \omega^3 B}{\omega^2 B^2 + k^2}\right) cos(\omega t) + \left(\frac{\omega^2 B^2 - I_m \omega^2 k + k^2}{\omega^2 B^2 + k^2}\right) sin(\omega t). \tag{2.6}$$

If we consider the extremes of equation (4.9), we can begin to draw conclusions about the motor requirements and relationships between the passive dynamic parameters. One extreme occurs when $B = 0$, and equation (4.9) simplifies to:

$$\tau_m(t) = \left(1 - \frac{I_m \omega^2}{k}\right) sin(\omega t). \tag{2.7}$$

Equation (4.10) implies that if the system has very little or no damping, the only way to reduce the torque requirement is to increase k or decrease I_m.

In contrast, if the system has very little or no elasticity, such that $k \approx 0$, (4.9) simplifies to:

$$\tau_m(t) = \left(\frac{I_m \omega}{B}\right) cos(\omega t) + sin(\omega t). \tag{2.8}$$

Equation (4.11) implies that to reduce the torque requirement, increasing B or decreasing I_m are the only options.

Comparing (4.10) and (4.11), we note that as the frequency increases, B has a much greater effect than k on reducing the required motor torque.

The graphs in Fig. 4.3 show the maximum frequency the system can achieve for a set of parameters k, B and I_m. We arbitrarily set $\tau_{limit} = 10$ for each graph and hold I_m constant for Fig. 4.3a and Fig. 4.3b. The graphs demonstrate the effects of modifying the various parameters of equation (4.9).

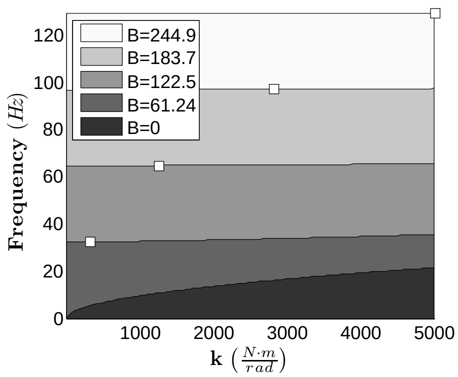

(a) : Frequency achieved vs. series elasticity, k. Increasing the elasticity slowly increases the maximum frequency.

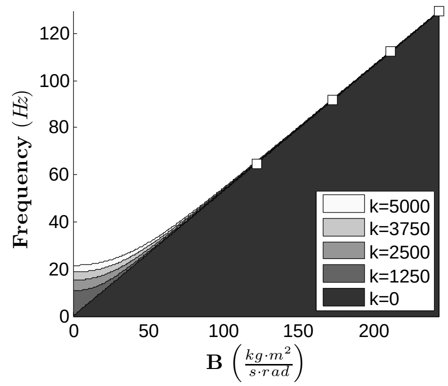

(b) : Frequency achieved vs. series damping, B. Increasing the damping increases the maximum frequency.

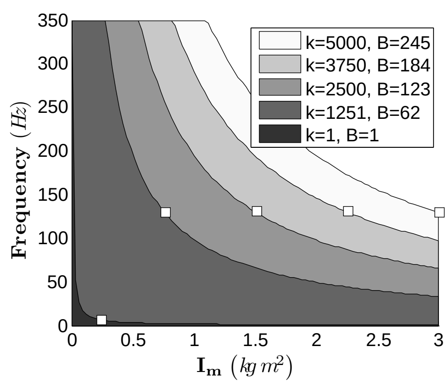

(c) : Frequency achieved vs. motor inertia, I_m. Increasing the inertia greatly decreases the maximum frequency.

Figure 2.3: Performance of the series elastic/damped actuator applying a sinusoidal torque against a stationary load (Fig. 4.2). The maximum frequency occurs at the point where the load torque error exceeds 0. For reference, the squares on each figure indicate where the system is critically damped. For figures 4.3a and 4.3b, $I_m = 3$.

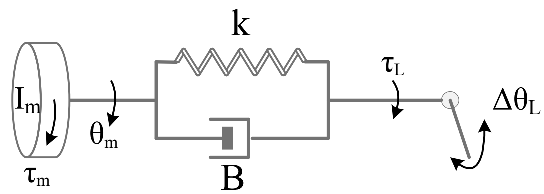

Figure 2.4: For the second scenario, the load is forced to move by θ_L while the motor attempts to keep the load torque, τ_L, zero with the passive dynamic elements k and B.

It follows from these equations that increasing stiffness provides higher bandwidth for applying varying torques to a fixed load. The equations indicate that there is an inverse relationship between the maximum frequency and the motor inertia (as shown in Fig. 4.3c). An increase in k or B will increase the bandwidth but an increase in I_m will decrease the bandwidth.

2.6 Zero torque against a moving load

The second task requires the actuator to maintain zero torque against a moving load (Fig. 4.4). We again demonstrate how k, B and I_m affect the maximum frequency, which we define for this task as the frequency at which the load position can oscillate before a prescribed torque error at the load is exceeded. This situation might occur if the goal of the actuator is to keep contact with an object, while maintaining a constant applied torque. An example of this task might be carrying a coffee cup while walking or the iso-elastic system in a Steadicam. Note that there is no inertia at the load, as its motion is predefined and is not affected by the applied torque.

We start by looking at the point where the torque required of the motor becomes greater than the torque limit. For this task we want to find the motor torque as a function of time, $\tau_m(t)$, for a predefined motion of the load, $\theta_L(t)$ and the desired load torque, $\tau_L(t)$. For this scenario, we hold the load torque constant at zero. We then define the desired load position to follow a sinusoidal function at some angular frequency, ω, and an amplitude of θ_A (Fig. 4.4)

$$\begin{aligned} \theta_L(t) &= \theta_A sin(\omega t) \\ \tau_L(t) &= 0. \end{aligned} \tag{2.9}$$

Taking the Laplace transform of $\theta_L(t)$ gives:

$$T_L(s) = \theta_A \frac{\omega}{s^2 + \omega^2}. \tag{2.10}$$

Plugging (4.13) back into (4.5) and taking the inverse Laplace transform we find the $\tau_m(t)$ required to produce the $\tau_L(t)$ defined in (4.12) at steady state ($t \gg 0$):

$$\tau_m(t) = \left(-\theta_A I_m \omega^2\right) sin(\omega t). \tag{2.11}$$

Intuitively this shows that for the motor to exactly produce zero torque at the load, it would have to generate a torque that would cause the motor position (θ_m) to exactly follow the load position (θ_L). We can also conclude that k and B do not matter when trying to follow the load motion. Instead, the only parameter we have for reducing the motor torque requirement is the motor inertia.

However, it may be more useful to measure the load torque within some error tolerance. To actually investigate how k and B affect the system, we now assume that there can be error in the load torque. To produce an error, we take the optimal output defined in (4.14) and clip it when the torque limits are encountered as shown in Fig. 4.5a.

With the limited τ_m as the input, we can find the response at τ_L. This new response contains an error for which we can choose a threshold based on system requirements. We can now use the error threshold as a metric for defining the maximum frequency the actuator can provide zero τ_L. The response now also depends on k and B. Fig. 4.5b shows an example of how τ_L responds to a limited τ_m.

To gain an understanding of how the actuator responds with different passive dynamic parameters, we present the graphs in Fig. 4.6. Notice that in this scenario, the maximum achievable frequencies quickly become relatively low even with modest values of k and B (Fig. 4.6a and Fig. 4.6b).

These graphs highlight the result that decreasing stiffness provides higher bandwidth for tracking the load motion, while maintaining acceptable output error. They also indicate that there is an inverse relationship between the maximum frequency, f_{max}, and the parameters, k, B and I_m. In other words, a decrease in k, B or I_m increases the bandwidth.

Even as the stiffness increases to infinity ($k, B \to \infty$), the maximum frequency will never dip below:

$$f_{worst} = \left(\frac{1}{2\pi}\right)\sqrt{\frac{\tau_{limit}}{\theta_A I_m}}. \tag{2.12}$$

Equation (4.15) was found by setting (4.14) equal to τ_{limit} and solving for frequency.

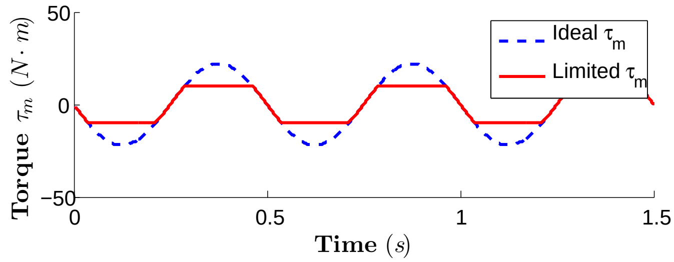

(a) : The input torque, τ_m. The ideal input represents what is needed to produce zero error. The limited input results from the torque limit being applied to the ideal input.

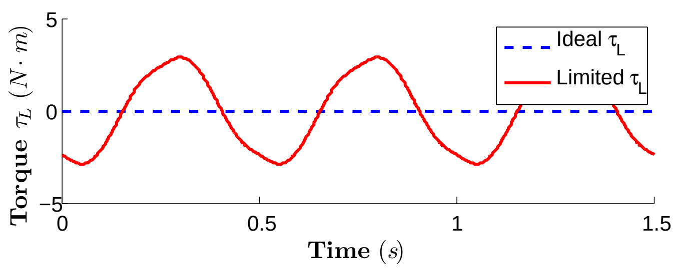

(b) : The resulting load torques from the inputs in Fig. 4.5a. Notice how the limited motor torque, τ_m, no longer generates zero torque at the load, τ_L.

Figure 2.5: Example load torque, τ_L, responses to an ideal and limited motor torque, τ_m, generated while attempting to apply zero torque against a moving load. $I_m = 0.4$, $k = 10$, $B = 1$ and $\tau_{limit} = 10$.

The frequency, f_{worst}, represents the maximum frequency the load motion can move at before the motor torque limit, τ_{limit}, is reached. For any frequency beyond f_{worst} there will be an error, whose magnitude depends on the inertia of the motor, k and B. This frequency is plotted as the dashed white line in Fig. 4.6a and Fig. 4.6b.

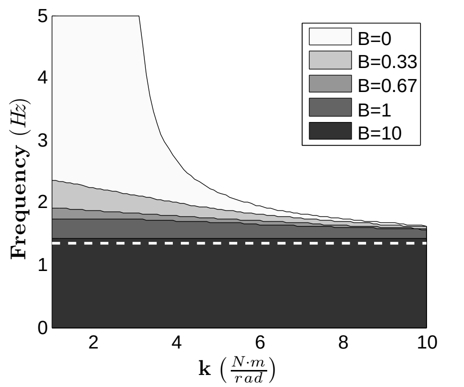

(a) : Frequency achieved vs. series elasticity, k. Increasing the elasticity decreases the maximum frequency.

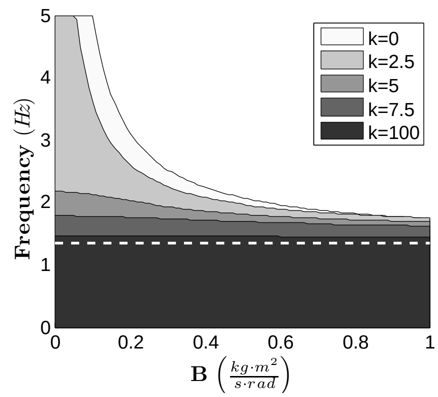

(b) : Frequency achieved vs. series damping, B. Increasing the damping decreases the maximum frequency.

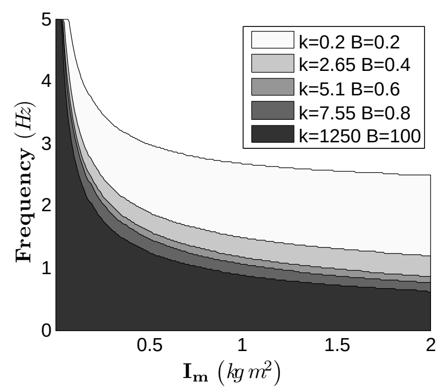

(c) : Frequency achieved vs. motor inertia, I_m. Increasing the motor inertia decreases the maximum frequency.

Figure 2.6: Performance of a series elastic/damped actuator applying zero torque against a moving load with some allowable error. The maximum frequency is the point where the load torque error exceeds 1 $N \cdot m$. The white dashed lines in figures 4.6a and 4.6b are the worst case maximum frequency, and occur when the system stiffness approaches infinity. For figures 4.6a and 4.6b, $I_m = 0.4$.

2.7 Conclusions and future work

In this paper, we derived the physical limitations of actuators with passive dynamics that can be described by the dynamic model shown in Fig. 4.1. Our model does

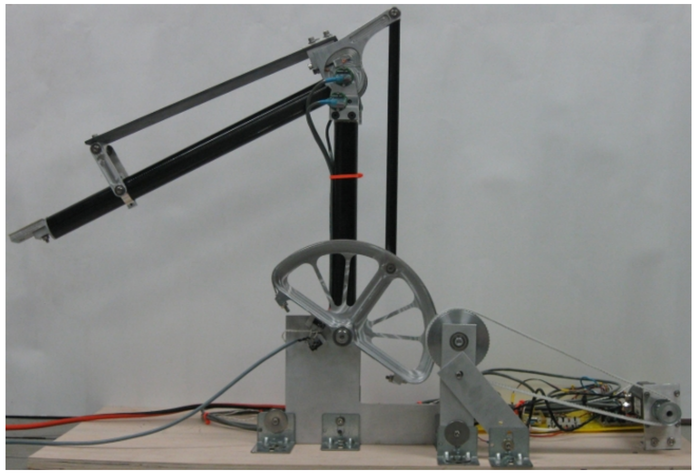

Figure 2.7: Test platform for a single degree of freedom force controlled actuator. The system tracks its output force by measuring the deflection in its spring. Springs of varying stiffness can quickly be interchanged.

not include active control; we computed the optimal input to the system to produce the required torque at the load with zero or acceptable error. This is important so that our results only reflect the physical system's performance. These exact solutions provide the basis for understanding how the parameters affect bandwidth and how to select parameters for a torque control task. Each of these tasks are designed to represent extreme applications of torque and force control.

For our model to generate a varying torque against a fixed load, the system should have higher stiffness and/or lower inertia. Perhaps less obvious is that both damping and inertia play a much larger role in increasing the maximum frequency than stiffness.

For the actuator to produce exactly zero torque against a moving load, the system's stiffness does not matter. Instead, the stiffness only determines how quickly the error increases with increased frequency. We found that reducing stiffness decreases error caused by motor torque limits. But as the stiffness approaches infinity, the performance of the actuator is governed solely by the motor inertia and torque limit.

It is evident that designing an actuator optimized for both varying torque against a stationary load and applying zero torque against a moving load, is very difficult. In fact, they require exact opposite optimizations and share no set of parameters that provide good results for both tasks. The only way to improve the bandwidth of both tasks simultaneously is to reduce the motor inertia or increase the torque limit. This implies that actuators designed to perform a wide set of tasks require variable impedance.

Additional work will include the development of relationships for more complex actuation scenarios such as stopping an inertia or mass with initial velocity, or commanding the actuator to behave like a spring. Real examples of these tasks are space ship docking and legged locomotion. This work will inform engineers and robot designers on the roles of elasticity and damping. They will provide insight into how each parameter contributes for complex motions.

The next step in our work is to validate the calculations presented on a real system. We have begun constructing an actuator that embodies the model presented in this paper (Fig. 3.8). Our goal is to develop guidelines to allow engineers to understand the compromises and requirements of the mechanical system for all types of robotic physical interaction tasks.

2.8 Acknowledgments

Thanks to Benjamin Goska for discussion and mathematical advice.

Chapter 3 – Optimal passive dynamics for physical interaction: catching a mass

For manipulation tasks in uncertain environments, passive dynamics can provide significant benefits. Traditionally, the design of actuators revolves around developing the best possible software control strategy. However, the passive dynamics of the mechanical system, including inertia, stiffness, damping and torque limits, often impose performance limitations that cannot be overcome with software control. Discussions about the passive dynamics are often imprecise, lacking comprehensive details about the physical limitations. In this paper, we develop relationships between an actuator's passive dynamics and the resulting performance, for the purpose of better understanding how to tune the passive dynamics for catching an unexpected object. We use a mathematically optimal controller subject to force limitations, to stop the incoming object without breaking contact and bouncing. This is important so that our results only reflect the physical system's performance.

3.1 Introduction

Robots excel at precise position control and are useful for tasks that make use of this ability, such as CNC machining. However, physical interaction tasks such as catching a ball, walking, running, grasping unknown objects, constrained contact and even simple force or torque control have historically been difficult for robots. Each of these tasks involve dynamic effects such as unexpected impacts and/or a significant transfer of kinetic energy between the robot and its environment. Animals far outperform robots at many of these tasks, and we contend that this is due to inherent mechanical limitations in traditional robotic mechanisms rather than software control inadequacies.

Consider a traditional industrial robot arm, powered by electric motors with large gear reductions and rigid links. The traditional approach to catching an object is to rely on complex vision systems to estimate the trajectory of the object and carefully match the velocity at the time of contact to avoid large impact forces. Because these systems require an enormous amount of information about the object prior to contact, these methods are not robust or practical for systems outside of the lab. Any error in these calculations can cause very large impact forces, possibly damaging transmissions. In the extreme case where no information is known about the object prior to contact the system must rely completely on software control and the mechanics of the actuator to control the response. However, the motors have inertia, which is amplified through the gearbox into a significant reflected inertia, and combines with torque limitations on the motors to limit the acceleration. These passive dynamics cannot be overcome using software control. If an object impacts the arm, such as a baseball, the motors will have no chance to respond, the arm will behave as a rigid inertial object and the software control will have no part in its dynamic response.

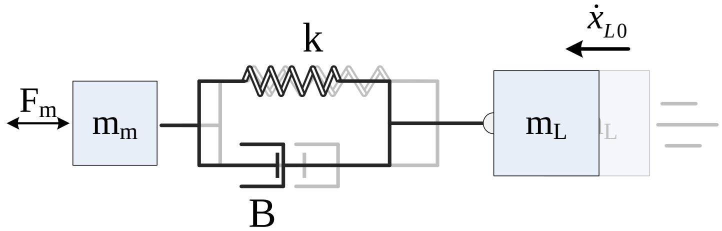

Figure 3.1: The system we investigate in this paper is entirely linear and includes damping, elasticity, motor inertia (represented as an equivalent mass) and motor force limits. Note that gravity does not apply to the motor mass.

Passive dynamics are not always harmful. As an example of passive dynamics improving performance, a mechanical spring in series with a motor can dramatically improve force control bandwidth in response to position disturbances, as exemplified by fishing rod. However, this improvement applies only to the specific case of force control and its robustness to position disturbances; a series spring will reduce the performance of the system for position control [17]. For peak performance in a robotic system, the passive dynamics must be tailored to the specific task. This is roughly analogous to impedance matching in electrical systems.

In this paper we define how an actuator's passive dynamics affect performance when experiencing an unexpected impact such as catching an object. We lay out a mathematical framework for mechanical systems that includes a motor with inertia and torque limits, a series spring and a series damper, as shown in Fig. 4.1.

We investigate the specific case of catching/stopping an unknown object without allowing it to bounce. We then describe the mathematically optimal passive dynamics required to achieve the best possible response, based on fundamental physical limits. Based on this and our previous work [17], roboticists will be able to design a mechanical system has the performance necessary for a particular task, especially tasks involving force or torque control, spring-like behavior, impacts and kinetic energy transfer.

3.2 Background

Muscular systems in animals incorporate elastic elements, which are most often examined while investigating locomotion, and are generally discussed in the context of energy storage [3][4] [5][6]. Roboticists have built machines designed to mimic this spring-like behavior [18] [8]. Although the designers of these running machines acknowledge that elasticity provides robustness, their studies generally focus on energy storage and efficiency. Little attention is given to how these elements contribute to general force control and manipulation with the environment.

Early investigations into force control found that series compliance in an actuator can increase stability, and in some cases is required for stable operation [10][9]. Researchers at the Massachusetts Institute of Technology (MIT) Leg Laboratory explored these ideas and created the Series Elastic Actuator (SEA). The MIT-SEA is designed specifically to include an elastic element as a force sensor and low impedance coupling between the drive system and the load to improve force control. It has been shown that this configuration provides filtering to handle shock loads and higher bandwidth force control [1][2]. The MIT-SEA offer great advantages, however, there has been no formal study of the performance on impacts such as catching unknown objects. Further work to improve the MIT-SEA has focused on control architecture

[12][11] or transmission design [19][14][13].

An extension MIT-SEA has been proposed by Hurst et al. [20]. They concluded that the added damping provides higher bandwidth than a purely series-elastic element and reduces unwanted oscillations in specific situations. Initial force spikes observed by the drive system at impact are greater than would be observed by just an elastic element, but are still much less than for a perfectly stiff system.

Discussions into how actuators behave when moving from free motion to a constrained contact (an impact) often focus on how to develop controllers to remove energy from the impact [21][22][23]. In all cases the authors acknowledge that the controllers are limited by the delay caused by the intrinsic mass and inertia even with perfectly fast physical collision detection. They avoid this issue though by limiting the investigation to the contact with soft, compliant types of surfaces [23] or rely on intrinsic (and uncharacterized) mechanical compliance in the design [22].

This paper builds on our previous investigation into how the passive dynamics of the physical system contribute to the performance of an actuator [17]. In that earlier work we described two actuation scenarios, position control and force control, and derived the relationship between physical damping and stiffness to the respective goals. We conclude that for an actuator to preform well at each task, mechanically variable impedance is necessary.

3.3 Problem domain

To develop the relationships between an actuator's design parameters, we investigate the series elastic/damping actuator (SEDA) in Fig. 3.2. Our actuator includes damping and elasticity because they are both physically unavoidable and possibly useful. We want to know how to select these elements (k and B) to design the best possible actuator around a force or torque control task.

In this paper, we define relationships between series stiffness, series damping, drive system inertia and the drive system torque limits in a specific experimental scenario. To simplify the discussion, we use "motor" to describe the drive system as a whole - transmission and motor characteristics. The following symbols describe our model:

k	Spring constant	$N \cdot m$
B	Damping constant	$\frac{N \cdot s}{m}$
g	Acceleration of gravity	$\frac{m}{s^2}$
m_m	Motor/transmission mass	kg
m_L	Load mass	kg
F_m	Motor force	N
F_{limit}	Motor force limit	N
F_g	Force due to gravity	N
F_d	Force caused by the dynamic elements	N
v_0	Load initial velocity	$\frac{m}{s}$

Our goal in this paper is to calculate the fundamental limitations of the physical

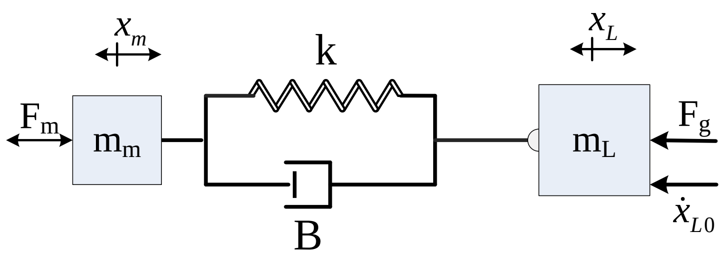

Figure 3.2: System schematic. The motor inertia is represented as a mass (m_m) with gravity (F_g) only acting on the load mass (m_L). This is analogous to an electric motor attached to a ballscrew transmission where the rotational inertia is much greater than the mass of the transmission itself. The load mass has initial velocity (v_0) at $t = 0$. The controlled input, F_m must be modulated such that spring never is in tension. If the spring is in tension then the load has lost contact with the actuator and the system has failed to catch the load.

system. Our model is controlled using a mathematically optimal controller. This is an important distinction from previous attempts to develop actuators of this nature. By eliminating controller error, we are able to isolate the physical limitations of our model.

In addition to the reactive elements k and B, we include motor force limits as well as motor inertia (represented as the mass m_m). If infinite force were possible, there would be no requirements for designing the impedance of the actuator. In other words, it would not matter how soft, or stiff, the elements were, just as long as they existed.

In the case of zero motor mass with motor force limits, the elastic and damping elements are no longer important. The elements just need to exist to provide for transmission of force. In this case the largest force the actuator could produce at the load would be the force limit, defining the maximum velocity and information is lost about how the dynamics effect the system. In either case the system is optimal, has infinite bandwidth for any task and the impedance of the actuator is irrelevant. Unfortunately, this is not the case with real systems because all motors have torque/force limits and rotor inertia and mass.

3.4 System model

To investigate how impacts, such as catching an unknown object, effect the actuator's behavior, we study the system shown in Fig. 3.2. This system is entirely linear with gravity only acting on the load. This is analogous to an electric motor attached to a ballscrew transmission where the rotational inertia is much greater than the mass of the transmission itself.

We start by defining the differential equations that describe the motion of the system:

$$[m]\begin{Bmatrix} \ddot{x}_L \\ \ddot{x}_m \end{Bmatrix} + [B]\begin{Bmatrix} \dot{x}_L \\ \dot{x}_m \end{Bmatrix} + [k]\begin{Bmatrix} x_L \\ x_m \end{Bmatrix} = \begin{Bmatrix} m_L g \\ F_m\left(t\right) \end{Bmatrix} \tag{3.1}$$

where

$$[B] = \begin{bmatrix} B & -B \\ -B & B \end{bmatrix} \tag{3.2}$$

$$[k] = \begin{bmatrix} k & -k \\ -k & k \end{bmatrix} \tag{3.3}$$

$$[m] = \begin{bmatrix} m_L & 0 \\ 0 & m_m \end{bmatrix}. \tag{3.4}$$

We define the performance of the system as the largest possible v_0 that the system can encounter without bouncing the incoming load, given a motor force limit. Therefore this problem cannot be expressed within the framework of classical optimal control theory (e.g. LQR) and we must simplify the system to develop the controller.

To simplify the system we can decouple (3.1) into two independent single degree of freedom (SODF) systems. Since the mode shapes are perpendicular to each other with respect to the mass, stiffness and damping matrices:

$$\{\phi\}_i^T [m] \{\phi\}_j = 0, \; i \neq j \tag{3.5}$$

$$\{\phi\}_i^T [k] \{\phi\}_j = 0, \; i \neq j \tag{3.6}$$

$$\{\phi\}_i^T [B] \{\phi\}_j = 0, \; i \neq j \tag{3.7}$$

we have

$$\begin{Bmatrix} x_L \\ x_m \end{Bmatrix} = \{\phi\}_1 z_1(t) + \{\phi\}_2 z_2(t). \tag{3.8}$$

This allows us to decouple the system by pre-multiplying both sides by $\{\phi\}_i^T$. We then can write a new set of equations describing the decoupled system as

$$(m_L + m_m)\,\ddot{z}_1(t) = m_L g + F_m(t) \tag{3.9}$$

$$m_e \ddot{z}_2(t) + B_e \dot{z}_2(t) + k_e z_2(t) = m_L g - \mu F_m(t) \tag{3.10}$$

where the equivalent parameters are

$$m_e = m_L(1+\mu) \tag{3.11}$$

$$B_e = B(1+\mu)^2 \tag{3.12}$$

$$k_e = k(1+\mu)^2 \tag{3.13}$$

$$\mu = \frac{m_L}{m_m}. \tag{3.14}$$

Equations (3.9) and (3.10) can be described in Fig. 3.3a and 3.3b respectively.

The two new models demonstrated in Fig. 3.3 are the two independent behaviors exhibited by the system. Fig. 3.3a represents the rigid body motion of the system and describes how the masses move together. Fig. 3.3b describes the oscillation of the masses relative to each other.

The boundary conditions for the initial system are

$$\begin{Bmatrix} x_L \\ x_m \end{Bmatrix}_{t=0} = \begin{bmatrix} 0 \\ 0 \end{bmatrix}, \begin{Bmatrix} \dot{x}_L \\ \dot{x}_m \end{Bmatrix}_{t=0} = \begin{bmatrix} v_0 \\ 0 \end{bmatrix}, \tag{3.15}$$

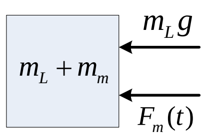

(a) : The rigid body motion of the system that describes how the masses move together.

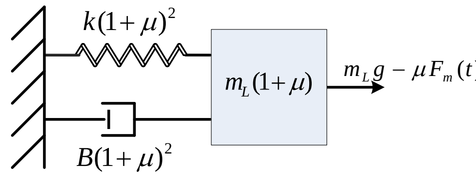

(b) : Equivalent oscillation of the masses relative to each other.

Figure 3.3: The original system in Fig. 3.2 can be broken into two separate single degree of freedom systems. Fig. 3.3a and 3.3a illustrate a physical representation of the new systems.

then the initial conditions for the new system become

$$z_1(0) = 0 \tag{3.16}$$

$$\dot{z}_1(0) = \frac{\mu v_0}{1+\mu} \tag{3.17}$$

$$z_2(0) = 0 \tag{3.18}$$

$$\dot{z}_2(0) = \frac{v_0}{1+\mu}. \tag{3.19}$$

The force generated by the dynamics is defined as

$$F_d(t) = B(\dot{x}_m - \dot{x}_L) + k(x_m - x_L). \tag{3.20}$$

This can be written in the new SDOF coordinate system by substituting (3.8) into (3.20):

$$F_d(t) = -B(1+\mu)\dot{z}_2(t) - k(1+\mu)z_2(t). \tag{3.21}$$

Equation (3.21) can be interpreted as the reaction force in Fig. 3.3b if the dynamics of the system is divided by $(1 + \mu)$.

$$m_L \ddot{z}_2 + B\,(1 + \mu)\,\dot{z}_2 + k\,(1 + \mu)\,z_2 = \frac{m_L g}{1 + \mu} - \frac{\mu F_m}{1 + \mu} \tag{3.22}$$

To keep the dynamic force $(F_d\,(t))$ always negative (the spring in compression), the support reaction in the equivalent SDOF has to be positive (or in tension) because of the minus sign in equation (3.21).

3.5 Controller

We are interested in how the passive dynamics and physical limitations influence the system so we must develop the best possible controller specifically for each configuration of system parameters. To catch the largest possible initial velocity, the actuator should dissipate as much energy as possible. To achieve that goal, the motor force must be at its limit away from the incoming load (Fig. 3.4a). When the equivalent mass reaches zero velocity, the motor force should switch directions and maintain maximum force as shown in Fig. 3.4b. By following this strategy, the largest possible initial velocity can be caught by the actuator given the limits. Figure 3.5 shows an example of the input force produced by the controller.

For our real system this is interpreted as applying the maximum force in the direction of gravity initially then applying the maximum force upward. The mass will not bounce if the actuator and damper are able to dissipate the whole initial velocity before the mass crosses the zero position.

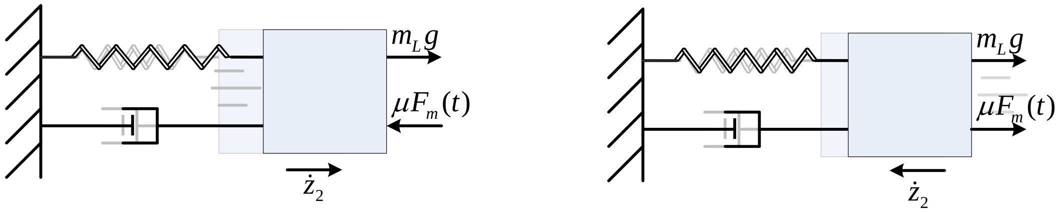

(a) : First stage of the controller. The equivalent mass initially moves toward the right with the controller pushing into the mass.

(b) : Second stage of the controller. When the equivalent mass begins to move back toward the initial position, the controller pulls on the mass to the right.

Figure 3.4: The first two phases of the controller. After these two phases, the load has been caught and simple position control can move the load to the desired position.

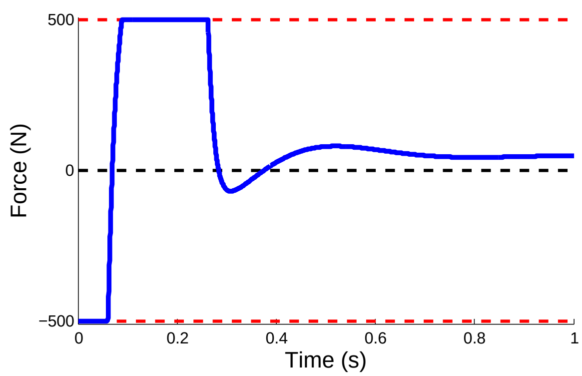

Figure 3.5: An example of the input force profile generated by the controller. In this case, the motor limit, F_{limit}, is 500 N.

3.6 Results

We can conclude that the softer spring, the larger the maximum initial velocity the system can catch. But it is often not plausible to use very soft spring because of inherent physical limitations like the spring deflection, actuator displacement and limitations of force applied to the load.

By decreasing the stiffness or damping, the maximum velocity that can be caught quickly increases. Figure 3.6a shows how damping and stiffness affect the maximum velocity that can be caught. An interesting note is that the effect of damping on softer springs is much more significant than on stiffer springs.

For a system without damping, the relation between the maximum possible initial velocity and maximum motor force as well as other mechanical properties of the system can be found by dissipating all of the kinetic energy of the system:

$$\frac{1}{2}m_L\left(\frac{v_0}{1+\mu}\right)^2 = 2\frac{\mu}{1+\mu}F_{limit}\ z_{2limit} \tag{3.23}$$

Where z_{2limit} is the maximum spring deflection. Solving (3.22) for the maximum z_2 with zero damping yields:

$$\begin{aligned} z_{2limit} &= \frac{1}{1+\mu}\left(\frac{F_{eq}}{k\left(1+\mu\right)}\right. \\ &\quad \left. +\sqrt{\left(\frac{v_0}{\omega}\right)^2+\left(\frac{F_{eq}}{k\left(1+\mu\right)}\right)^2}\right) \end{aligned} \tag{3.24}$$

where ω is the frequency of the equivalent SDOF system and F_{eq} is the equivalent force from Fig. 3.3b:

$$\omega = \sqrt{\frac{k\left(1+\mu\right)}{m_L}},\ F_{eq} = m_L g - \mu F_{limit} \tag{3.25}$$

After some simplification of (3.23) with (3.25) and (3.25), the maximum velocity that can be caught by a non-damped system can be obtained as:

$$v_0 = \sqrt{\frac{8F_{limit}\left(m_L g + \frac{m_L}{m_m}F_{limit}\right)}{k\left(m_L + m_m\right)}} \tag{3.26}$$

Solving (3.26) for F_{limit}, we can find the minimum motor force limit required to catch a mass with initial velocity v_0:

$$F_{limit} = \frac{\sqrt{\left(8m_L g\right)^2 + 32km_L\left(1+\mu\right)v_0^2} - 8m_L g}{16\mu} \tag{3.27}$$

If the above force (F_{limit}) cannot be provided, we will absolutely need at least some damping to catch the load. This can be observed in Fig. 3.6a where, if the system design requires v_0 of at most 20 $\frac{m}{s}$ then for $k = 2000$ $\frac{N}{m}$ we at least need damping of greater than about 40 $\frac{N \cdot s}{m}$ to stop the load without bouncing.

An important issue is the peak force that can be safely applied to the load by the actuator. The relation between the peak force and the dynamic elements is presented in Fig. 3.6b. At first glance it would appear that the graph is suggesting that as the stiffness of the system increases, the peak force on the load decreases. But consider that as the stiffness increases, the maximum initial velocity that the system can catch decreases.

In Fig. 3.7a, the effect of stiffness and damping on the maximum deflection of the spring is demonstrated. For stiff systems, adding damping has little effect on the maximum displacement of the spring. Because the spring deflection is one of the inherent physical properties of the mechanism, the design process can be

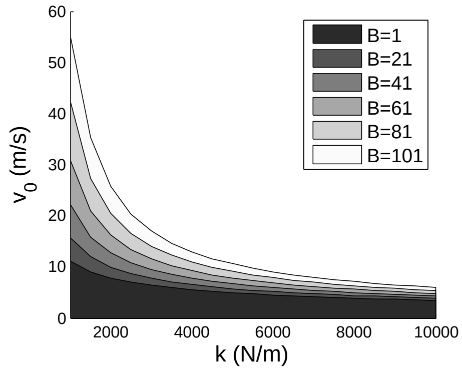

(a) : Maximum v_0 vs. series elasticity, k. Increasing the stiffness decreases the maximum incoming velocity the actuator can catch.

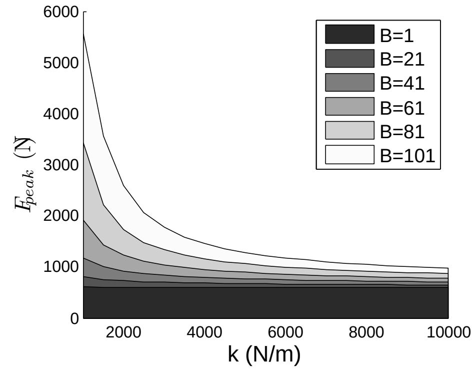

(b) : Maximum v_0 vs. series elasticity, k. Increasing the stiffness decreases the peak force applied to the load.

Figure 3.6: Performance of the series elastic/damped actuator while successfully stopping the load without bouncing. In each case, increasing the damping has a larger effect on the performance for softer springs. Overall performance decreasing as stiffness increases. For each figure, $m_m = m_L = 10$ and $F_{limit} = \pm 500$.

started from here to see in which range of the stiffness should be evaluated. For example, for spring deflection limit around 20 cm, no stiffness less than 3000 $\frac{N}{m}$ can be considered for catching the largest possible velocity shown in Fig. 3.6a. If both stiffness and displacement are fixed then the motor force limit must increase or the motor mass/inertia must change.

Maximum actuator motion is another physical limitation. The graph in Fig. 3.7b shows the peak motor displacement with respect to damping and stiffness of the system. For a maximum motor translation of around 50 cm, the spring should be at least as stiff as 4700 $\frac{N}{m}$ to catch the largest possible velocity.

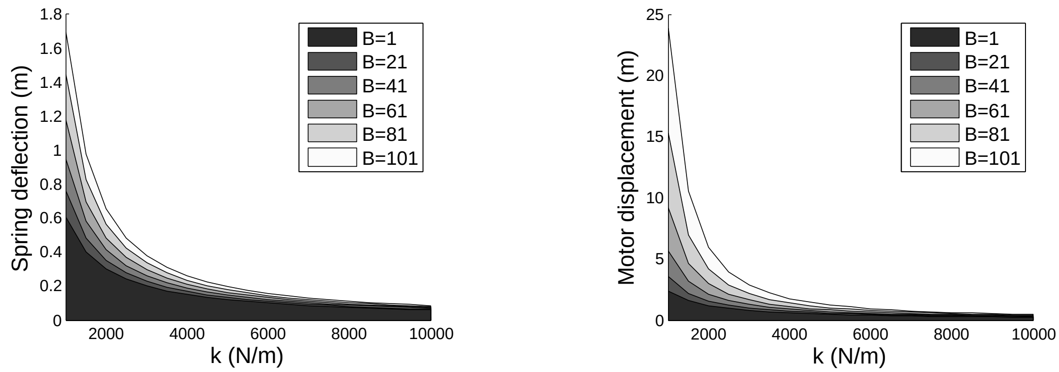

(a) : The minimum spring length required to catch the load with the maximum possible velocity. As the stiffness increases, the required length decreases.

(b) : The minimum motor travel required to catch the load. To be able to stop the maximum velocity, the system should be very soft but the motor must then be allowed to travel very far.

Figure 3.7: Performance of the series elastic/damped actuator while successfully stopping the load without bouncing. For each figure, $m_m = m_L = 10$ and $F_{limit} = \pm 500$.

3.7 Conclusions and future work

In this paper, we derived the physical limitations of actuators with passive dynamics that can be described by the model shown in Fig. 4.1. We defined relationships between series stiffness, series damping, drive system inertia and the drive system torque limits in a specific experimental scenario shown in Fig. 3.2.

We are interested in how the passive dynamics and physical limitations influence the system, so we compute the best possible controller specifically for each configuration of system parameters. This is important so that our results only reflect the physical system's performance. These optimal solutions provide the basis for understanding how the parameters affect the actuators ability to catch a load or manage an impact.

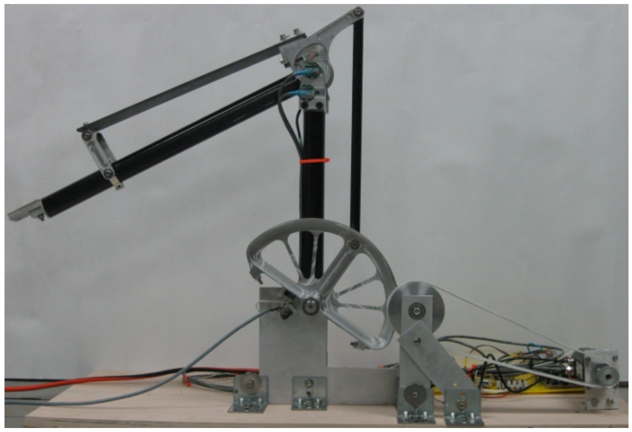

Figure 3.8: Test platform for a single degree of freedom force controlled actuator. The system tracks its output force by measuring the deflection in its spring. Springs of varying stiffness can quickly be interchanged.

We show that by decreasing the stiffness or damping, the maximum velocity that can be caught quickly increases. An interesting note is that the effect of damping on softer springs is much more significant than for stiffer springs. Adding damping has decreasing effect on the maximum displacement of the spring.

There are distinct trade-offs between catching a load with the maximum possible initial velocity and the distances the actuator or spring must travel. To optimize the initial velocity, the designer must decrease the stiffness and damping. However, as the dynamics become softer, the distance that the spring must deflect or that the motor must displace become proportionally larger. This compromise is an important consideration when designing a real physical system.

Additional work will include the development of relationships for more complex actuation scenarios such as commanding the actuator to behave like a spring or throwing a mass with maximum velocity. Real examples of these tasks are legged locomotion or novel material handling tasks in factories. This work will inform engineers and robot designers on the roles of elasticity and damping. They will provide insight into how each parameter contributes for complex motions.

The next step in our work is to validate the calculations presented on a real system. We have begun constructing an actuator that embodies the model presented in this paper (Fig. 3.8). Our goal is to develop guidelines to allow engineers to understand the compromises and requirements of the mechanical system for all types of robotic physical interaction tasks.

Chapter 4 – Optimal passive dynamics for continuous contact physical interaction

For robotic manipulation tasks in uncertain environments, research typically revolves around developing the best possible software control strategy. However, the passive dynamics of the mechanical system, including inertia, stiffness, damping and torque limits, often impose performance limitations that cannot be overcome with software control. Discussions about the passive dynamics are often imprecise, lacking comprehensive details about the physical limitations. In the first half of this paper, we develop relationships between an actuator's passive dynamics and the resulting performance, to better understanding how to tune the passive dynamics. We characterize constant-contact physical interaction tasks into two different tasks that can be roughly approximated as force control and position control and calculate the required input to produce a desired output. These exact solutions provide a basis for understanding how the parameters of the mechanical system affect the overall system's bandwidth limit without limitations of a specific control algorithm. We then present our experimental results compared to the analytical prediction for each task using a bench top actuator. Our analytical and experimental results show what, until now, has only been intuitively understood: soft systems

are better at force control, stiff systems are better at position control, and there is no way to optimize an actuator for both tasks. Thus, a robot that must do both tasks must be designed with variable impedance.

4.1 Introduction

Robots excel at precise position control and are useful for tasks that make use of this ability, such as CNC machining. However, physical interaction tasks such as catching a ball, walking, running, grasping unknown objects, constrained contact and even simple force or torque control have historically been difficult for robots. Each of these tasks involve dynamic effects such as unexpected impacts and/or a significant transfer of kinetic energy between the robot and its environment. Animals far outperform robots at many of these tasks, and we contend that this is due to inherent mechanical limitations in traditional robotic mechanisms rather than software control inadequacies. This paper focuses on how an actuator's passive dynamics affect its bandwidth performance in continuous-contact physical interaction.

Consider a traditional industrial robot arm, powered by electric motors with large

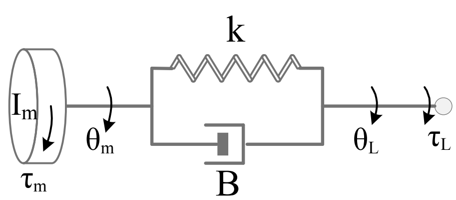

Figure 4.1: The system we investigate in this paper is entirely rotational and includes damping, elasticity, motor inertia and torque limits. The actuator is constrained such that only θ_m and θ_L can move.

gear reductions and rigid links. The traditional approach to force control utilizes such an arm, with a force sensor placed at the end-effector. Forces are measured, software controllers calculate the desired motor torques and the motors move accordingly. However, the motors have inertia, which is amplified through the gearbox into a significant reflected inertia, and combines with torque limitations on the motors to limit their acceleration. These passive dynamics cannot be overcome using software control. If an object impacts the arm, such as a baseball, the motors will have no chance to respond, the arm will behave as a rigid inertial object and the software control will have no part in its initial dynamic response.

Passive dynamics are not always limiting. As an example of passive dynamics improving performance, a mechanical spring in series with a motor can dramatically improve force control bandwidth in response to position disturbances. However, this improvement applies only to the specific case of force control and its robustness to position disturbances; a series spring will reduce the performance of the system for strict position control. For peak performance in a robotic system, the passive dynamics must be tailored to the specific task.

In this paper, we lay out a mathematical framework for mechanical systems that includes a motor with inertia and torque limits, a series spring and a series damper, as shown in Fig. 4.1. We investigate two examples; applying constant force to a moving object and applying changing force to a stationary object. We then describe the mathematically optimal passive dynamics required to achieve the best possible bandwidth, based on fundamental physical limits. We analytically show that a very compliant system is ideal for applying constant forces to moving objects (roughly analogous to force control), and a very stiff system is ideal for applying changing forces to a stationary object (roughly analogous to position control).

Humans are able to achieve a wide range of physical interaction tasks, including freehand machining of wood and riding in a car without spilling a cup of coffee, because they actively change the passive dynamic properties of their arm through co-contraction of antagonistic muscles. When using a router to machine wood, the woodworker's muscles are tensed, and his arm is as rigid and stiff as he can make it; and even so, the performance is much lower than a much more rigid CNC machine. In contrast, when stabilizing a cup of coffee, the passenger's arm largely relaxes reducing the arm stiffness; even so, the performance is much lower than a much less stiff Steadicam camera stabilization rig.

The final section of this paper experimentally validates the theory using three different sets of system parameters. Based on this work, roboticists will be able to calculate the bandwidth that is achievable for a specific mechanical system engaging in a particular constant-contact physical interaction task.

4.2 Background

Muscular systems in animals incorporate elastic elements, which are most often examined while investigating locomotion, and are generally discussed in the context of energy storage [3, 4, 5, 6]. Roboticists have built machines designed to mimic this spring-like behavior [8, 18]. Although the designers of these running machines acknowledge that elasticity provides robustness, their studies generally focus on energy storage and efficiency, with little attention to force control.

Early investigations into force control found that series compliance in an actuator can increase stability, and in some cases is required for stable operation [9, 10]. Researchers at the Massachusetts Institute of Technology (MIT) Leg Laboratory explored these ideas and created an actuator designed specifically to include an elastic element as a force sensor and low impedance coupling between the drive system and the load to improve force control. The system is aptly dubbed a series elastic actuator (MIT-SEA) and it has been shown that this configuration provides filtering to handle shock loads as well as higher bandwidth force control [1, 2]. MIT-SEAs offer great advantages, however, there are only approximate guidelines for choosing an appropriate spring. Further work to improve the MIT-SEA has focused on control architecture [11, 12] or transmission design [13, 14].

An actuator design using a viscous damper in place of the elastic element, dubbed a series damper actuator (SDA) has been proposed by Chew et al. [15]. They hypothesize that using damping, rather than elasticity, allows for greater bandwidth, and can be easily constructed to allow a variable damping coefficient. They admit that the main disadvantage of the SDA is the energy dissipation property, which limits the energy efficiency of the design. The developers of the SDA do not provide concrete relationships between damping and bandwidth, but present a conjecture relating the two.

Other groups have acknowledged that there are mechanical limits of low impedance actuators and have presented novel actuation techniques to overcome them. Several such designs have been summed up in [24]. In all cases it is clear the that the designs are motivated by the need for stiff systems under certain tasks while trying to preserve the benefits that low impedance provides for human interaction and force control. However, each of the groups only present mechanisms for changing stiffness and do not explicitly address how to choose a particular stiffness.

For an entirely different approach, Zinn et al. proposed using two actuators in parallel overcome the limits [25]. They use a lower inertia, lower power actuator to produce the high frequency forces needed for good disturbance rejection in parallel to a traditional SEA used to produce the larger, lower frequency torques. They demonstrate that this approach can improve the performance an SEA but do not describe the effects of damping or the magnitude of stiffness needed for the goals of their actuator.

A hybrid of the SDA and MIT-SEA has been proposed by Hurst et al. [20]. They concluded that the added damping provides higher bandwidth than a purely series-elastic element and reduces unwanted oscillations in specific situations. Initial force spikes observed by the drive system at impact are greater than would be observed by just an elastic element, but are still much less than for a perfectly stiff system.

4.3 System model

In this paper, we define relationships between series stiffness, series damping, drive system inertia and the drive system torque limits in specific experimental scenarios. To simplify the discussion, we use “motor” to describe the drive system as a whole - transmission and motor characteristics. The symbols in table 4.1 describe our model.

Our goal in this paper is to calculate the fundamental limitations of the physical system. Our model does not include active control; we compute the optimal input to the system to produce a desired torque at the load. This is an important distinction from previous attempts to develop actuators of this nature. By eliminating controller error, we are able isolate the physical limitations of our model.

To develop the relationships between an actuator's design parameters, we investigate the series elastic/damping actuator (SEDA) in Fig. 4.1. Our actuator includes damping and elasticity because they are both physically unavoidable and possibly useful. We want to know how to select these elements (k, β and I_m) to design the best possible actuator around a force or torque control task.

Our system model is entirely rotational because our lab, the Dynamic Robotics Laboratory, is interested in developing robots that use electric motors. However, the concepts in this paper relate directly to force control as well as to torque control. Roboticists designing actuators with linear drive systems (such as hydraulic pistons) can use the relationships presented in this paper to develop linear systems.

k	Spring constant	$\frac{N \cdot m}{rad}$
β	Damping constant	$\frac{kg \cdot m^2}{s \cdot rad}$
I_m	Motor inertia	$kg \cdot m^2$
τ_m	Motor torque	$N \cdot m$
τ_{limit}	Motor torque limit	$N \cdot m$
τ_L	Load torque	$N \cdot m$
θ_m	Motor angle	rad
θ_L	Load angle	rad
θ_A	Load angle amplitude	rad

Table 4.1: List of the common variables and notation used in this paper.

In addition to the reactive elements k and β, we include motor torque limits as well as motor inertia. The torque limit and motor inertia are important for the calculation of the bandwidth. If infinite torque were possible, there would be no requirements for designing the impedance of the actuator. In other words, it would not matter how soft, or stiff, the elements were, just as long as they existed.

In the case of zero motor inertia with motor torque limits, the elastic and damping elements are no longer important. The elements just need to exist to provide for transmission of torque. In this case the largest torque the actuator could produce at the load would be the torque limit. In either case the system is optimal, has infinite bandwidth for any task and the impedance of the actuator is irrelevant. Unfortunately, this is not the case with real systems because all motors have torque limits and rotor inertia.

4.4 Mathematical approach

Each scenario is designed to show that there is an optimal relationship between k, β and I_m for a distinct task. This paper focuses on simple, fundamental motions that might be expected from a force or torque controlled actuator. The goal is to relate k, β, I_m and τ_{limit} to the performance of a robotic actuator under specific conditions.

To determine the effect of k, β and I_m on the performance of the system in any test scenario, we first solve for the motor torque, τ_m, that produces the desired load torque, τ_L. If τ_m remains below the motor's peak torque limit, the system is able to achieve the desired performance goals.

In most cases, as the frequency of a task increases, the required motor torque increases and eventually meets the motor torque limit. The function for the exact motor torque, evaluated with torque limits, becomes the basis for describing the relationships that parameters have on achieving the maximum frequency of each task.

To find the required motor torque, we start by defining the differential equations that describe the motion of the system:

$$I_m\ddot{\theta}_m = \tau_m - \tau_\beta - \tau_k \tag{4.1}$$

$$0 = \tau_\beta + \tau_k - \tau_L \tag{4.2}$$

where:

$$\tau_k = k[\theta_m - \theta_L] \tag{4.3}$$

$$\tau_\beta = \beta[\dot{\theta}_m - \dot{\theta}_L]. \tag{4.4}$$

We then take the Laplace transform of (4.1) and (4.2), and solve for the s-domain equation of the motor torque ($T_m(s)$). With initial conditions ignored, this is calculated as:

$$T_m(s) = \Theta_L(s)\left(I_m s^2\right) + T_L(s)\left(\frac{I_m s^2 + \beta s + k}{\beta s + k}\right). \tag{4.5}$$

Equation (4.5) describes how the load motion and desired load torque affect the required motor torque, where $\Theta_L(s)$ is the s-domain representation of the load motion and $T_L(s)$ is the s-domain representation of the load torque. With this equation, we can define any motion for the load and a desired load torque and determine the exact requirement for the motor torque. At steady state, this computed motor torque will produce the torque at the load with zero error.

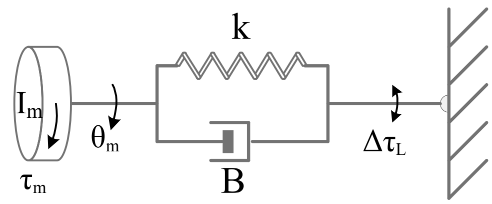

Figure 4.2: For the first scenario, the load is fixed to ground ($\theta_L = 0$) while the motor attempts to produce the desired τ_L through the passive dynamic elements k and β.

4.5 Changing torque against a static surface

For the first task, our model applies a sinusoidal torque to a fixed load (Fig. 4.2). We demonstrate how k, β and I_m affect the maximum frequency at which the actuator can vary the applied torque. The maximum frequency for this case is defined as the frequency that the actuator can oscillate the torque at the load before steady-state error is encountered.

To evaluate the maximum frequency the actuator can achieve under a given set of values for k, β and I_m, we consider the point where the motor's torque becomes greater than the torque limit. At this point the motor is no longer able to produce the required torque to exactly generate the desired τ_L.

To find the motor torque as a function of time, $\tau_m(t)$, we define the motion of the load, $\theta_L(t)$ and the desired load torque, $\tau_L(t)$. For this scenario, we hold the load position constant (Fig. 4.2). We then define the desired load torque to be a sinusoidal function with some angular frequency, ω, and a fixed amplitude of 1 $N \cdot m$. Note that the amplitude can be greater or smaller without affecting the relationships as long as it is less than the torque limit:

$$\theta_L(t) = 0 \tag{4.6}$$

$$\tau_L(t) = sin(\omega t). \tag{4.7}$$

Taking the Laplace transform of $\tau_L(t)$ gives:

$$T_L(s) = \frac{\omega}{s^2 + \omega^2}. \tag{4.8}$$

Plugging equation (4.8) back into (4.5) and taking the inverse Laplace transform, we find the $\tau_m(t)$ required to produce the $\tau_L(t)$ defined in (4.7) at steady state $(t \gg 0)$:

$$\tau_m(t) = \left(\frac{I_m \omega^3 \beta}{\omega^2 \beta^2 + k^2}\right) cos(\omega t) + \left(\frac{\omega^2 \beta^2 - I_m \omega^2 k + k^2}{\omega^2 \beta^2 + k^2}\right) sin(\omega t). \tag{4.9}$$

If we consider the extremes of equation (4.9), we can begin to draw conclusions about the motor requirements and relationshipsbetween the passive dynamic parameters. One extreme occurs when $\beta = 0$, and equation (4.9) simplifies to:

$$\tau_m(t) = \left(1 - \frac{I_m \omega^2}{k}\right) sin(\omega t). \tag{4.10}$$

Equation (4.10) implies that if the system has very little or no damping, the only way to reduce the torque requirement is to increase k or decrease I_m.

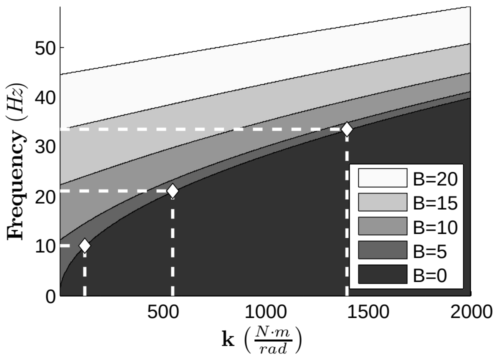

(a) Frequency achieved vs. series elasticity, k. Increasing the elasticity slowly increases the maximum frequency.

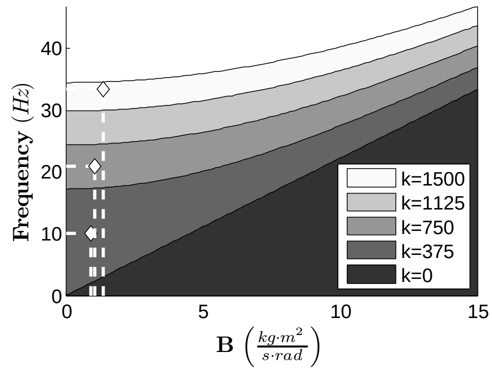

(b) Frequency achieved vs. series damping, β. Increasing the damping increases the maximum frequency.

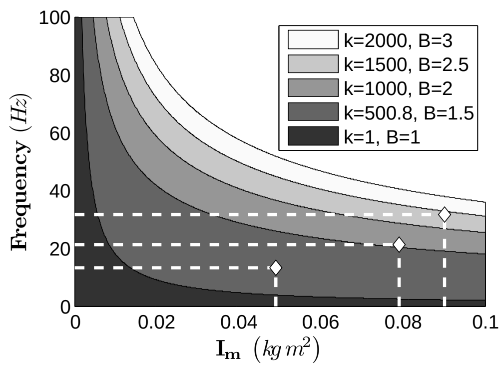

(c) Frequency achieved vs. motor inertia, I_m. Decreasing the inertia greatly increases the maximum frequency.

Figure 4.3: Performance of the series elastic/damped actuator applying a sinusoidal torque against a stationary load (Fig. 4.2). The maximum frequency occurs at the point where the load torque error exceeds 0. For reference, the diamonds on each figure indicate the theoretical performance of the experimental springs using the . For figures 4.3a and 4.3b, $I_m = 0.08\ kg\, m^2$ and $\tau_{limit} = \pm 15\ N \cdot m$.

In contrast, if the system has very little or no elasticity, such that $k \approx 0$, (4.9) simplifies to:

$$\tau_m(t) \;=\; \left(\frac{I_m \omega}{\beta}\right) cos(\omega t) + sin(\omega t). \tag{4.11}$$

Equation (4.11) implies that to reduce the torque requirement, increasing β or decreasing I_m are the only options.

Comparing (4.10) to (4.11), we note that as the frequency increases, β has a much greater effect than k on reducing the required motor torque.

The graphs in Fig. 4.3 show the maximum frequency the system can achieve for a set of parameters k, β and I_m. We arbitrarily set $\tau_{limit} = 10$ for each graph and hold I_m constant for Fig. 4.3a and Fig. 4.3b. The graphs demonstrate the effects of modifying the various parameters of equation (4.9).

It follows from these equations that increasing stiffness provides higher bandwidth for applying varying torques to a fixed load. The equations indicate that there is an inverse relationship between the maximum frequency and the motor inertia (as shown in Fig. 4.3c). An increase in k or β will increase the bandwidth but an increase in I_m will decrease the bandwidth.

4.6 Zero torque against a moving load

The second task requires the actuator to maintain zero torque against a moving load (Fig. 4.4). We again demonstrate how k, β and I_m affect the maximum frequency, which we define for this task as the frequency at which the load position can oscillate

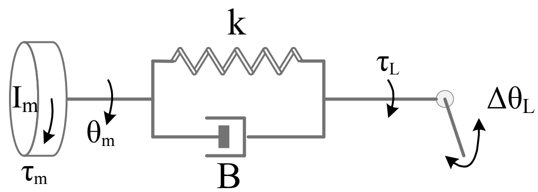

Figure 4.4: For the second scenario, the load is forced to move by θ_L while the motor attempts to keep the load torque, τ_L, zero with the passive dynamic elements k and β.

before a prescribed torque error at the load is exceeded. This situation might occur if the goal of the actuator is to keep contact with an object, while maintaining a constant applied torque. An example of this task might be carrying a coffee cup while walking or the iso-elastic system in a Steadicam. Note that there is no inertia at the load, as its motion is predefined and is not affected by the applied torque.

We start by looking at the point where the torque required of the motor becomes greater than the torque limit. For this task we want to find the motor torque as a function of time, $\tau_m(t)$, for a predefined motion of the load, $\theta_L(t)$ and the desired load torque, $\tau_L(t)$. For this scenario, we hold the load torque constant at zero. We then define the desired load position to follow a sinusoidal function at some angular frequency, ω, and an amplitude of θ_A (Fig. 4.4)

$$\begin{aligned} \theta_L(t) &= \theta_A sin(\omega t) \\ \tau_L(t) &= 0. \end{aligned} \tag{4.12}$$

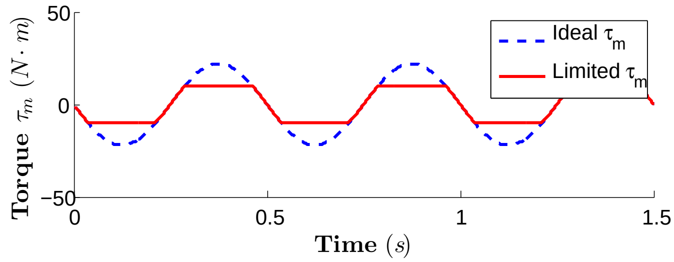

(a) The input torque, τ_m. The ideal input represents what is needed to produce zero error. The limited input results from the torque limit being applied to the ideal input.

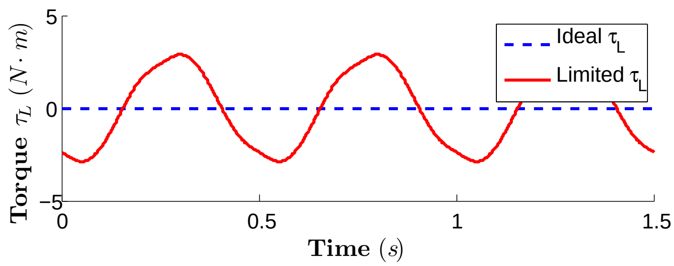

(b) The resulting load torques from the inputs in Fig. 4.5a. Notice how the limited motor torque, τ_m, no longer generates zero torque at the load, τ_L.

Figure 4.5: Example load torque, τ_L, responses to an ideal and limited motor torque, τ_m, generated while attempting to apply zero torque against a moving load. $I_m = 0.4$, $k = 10$, $\beta = 1$ and $\tau_{limit} = 10$.

Taking the Laplace transform of $\theta_L(t)$ gives:

$$\Theta_L(s) \quad = \quad \theta_A \frac{\omega}{s^2 + \omega^2}. \tag{4.13}$$

Plugging (4.13) back into (4.5) and taking the inverse Laplace transform we find the $\tau_m(t)$ required to produce the $\tau_L(t)$ defined in (4.12) at steady state ($t \gg 0$):

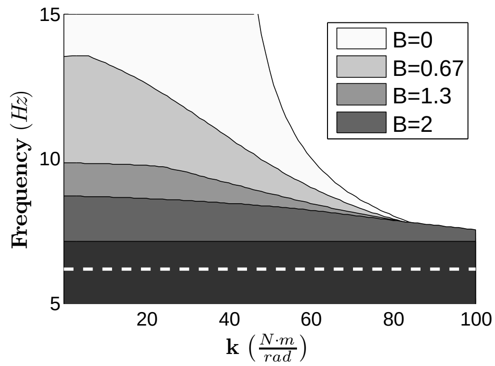

(a) Frequency achieved vs. series elasticity, k. Decreasing the elasticity increases the maximum frequency.

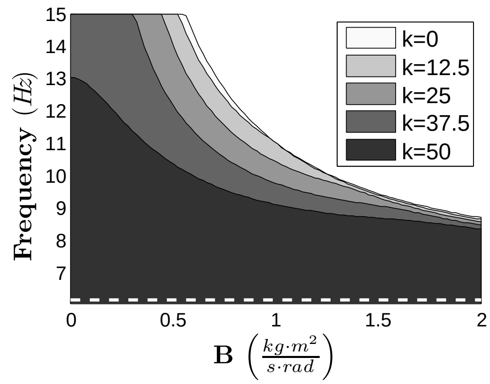

(b) Frequency achieved vs. series damping, β. Decreasing the damping increases the maximum frequency.

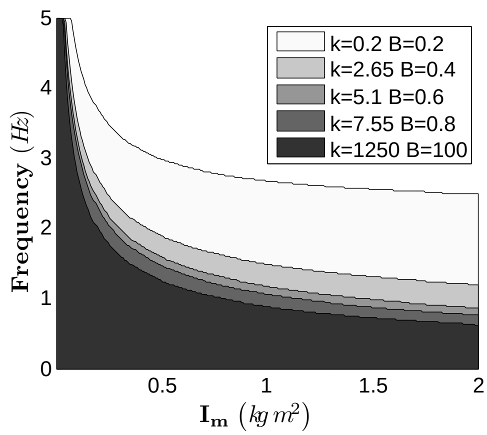

(c) Frequency achieved vs. motor inertia, I_m. Decreasing the motor inertia increases the maximum frequency.

Figure 4.6: Performance of a series elastic/damped actuator applying zero torque against a moving load with some allowable error. The maximum frequency is the point where the load torque error exceeds 1 $N \cdot m$. The white dashed lines in figures 4.6a and 4.6b are the worst case maximum frequency, and occur when the system stiffness approaches infinity. For figures 4.6a and 4.6b, $I_m = 0.4$.

$$\tau_m(t) \;=\; \left(-\theta_A I_m \omega^2\right) sin(\omega t). \tag{4.14}$$

Intuitively this shows that for the motor to exactly produce zero torque at the load, it would have to generate a torque that would cause the motor position (θ_m) to exactly follow the load position (θ_L). We can also conclude that k and β do not matter when trying to follow the load motion. Instead, the only parameter we have for reducing the motor torque requirement is the motor inertia.

However, it may be more useful to measure the load torque within some error tolerance. To actually investigate how k and β affect the system, we now assume that there can be error in the load torque. To produce an error, we take the optimal output defined in (4.14) and clip it when the torque limits are encountered as shown in Fig. 4.5a.

With the limited τ_m as the input, we can find the response at τ_L. This new response contains an error for which we can choose a threshold based on system requirements. We can now use the error threshold as a metric for defining the maximum frequency the actuator can provide zero τ_L. The response now also depends on k and β. Fig. 4.5b shows an example of how τ_L responds to a limited τ_m.

To gain an understanding of how the actuator responds with different passive dynamic parameters, we present the graphs in Fig. 4.6. Notice that in this scenario, the maximum achievable frequencies quickly become relatively low even with modest values of k and β (Fig. 4.6a and Fig. 4.6b).

These graphs highlight the result that decreasing stiffness provides higher bandwidth for tracking the load motion, while maintaining acceptable output error. They also indicate that there is an inverse relationship between the maximum frequency, f_{max}, and the parameters, k, β and I_m. In other words, a decrease in k, β or I_m increases the bandwidth.

Even as the stiffness increases to infinity ($k, \beta \to \infty$), the maximum frequency will never dip below:

$$f_{worst} = \left(\frac{1}{2\pi}\right)\sqrt{\frac{\tau_{limit}}{\theta_A I_m}}. \tag{4.15}$$

Equation (4.15) was found by setting (4.14) equal to τ_{limit} and solving for frequency.

The frequency, f_{worst}, represents the maximum frequency the load motion can move at before the motor torque limit, τ_{limit}, is reached. For any frequency beyond f_{worst} there will be an error, whose magnitude depends on the inertia of the motor, k and β. This frequency is plotted as the dashed white line in Fig. 4.6a and Fig. 4.6b.

4.7 Experimental setup

To validate the theoretical limits determined in the previous sections we have conducted experiments with the series elastic actuator in Fig. 4.7. Different springs can easily be swapped into the actuator. To determine the spring function for each fiberglass plate-spring, we command the motor through a series of constant torques, sampling the spring's deflection after settling. From the measured data we found simple linear approximations, rounding them to the nearest convenient value. Plots

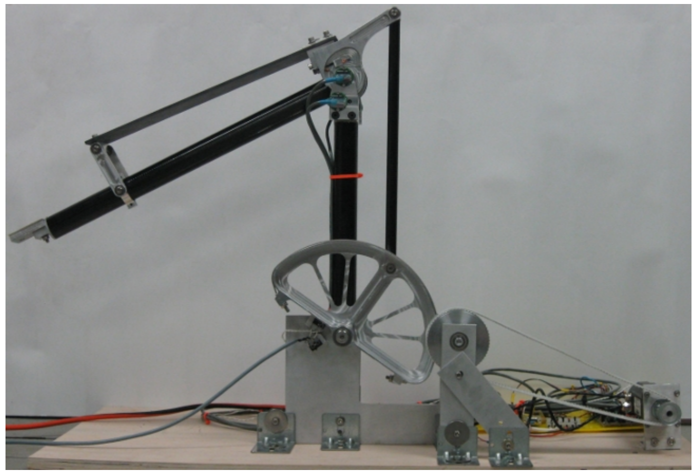

Figure 4.7: The actuator developed to examine force control tasks. The mechanism uses a fiberglass plate-spring in between the end-effector and brushless DC motor.

of each spring's measured and approximated displacement verses torque are shown in Fig. 4.8.

To determine the unknown system properties (β and I_m) each spring was held flexed as far as the motor torque allowed. The motor power was then cut allowing the spring to oscillate the mechanism until friction finally stopped the system. We then fitted a simple spring-mass-damper oscillator to the measured data using the spring constant derived in Fig. 4.8. An example of the simulated system plotted onto the measured response of the stiffest spring is demonstrated in Fig. 4.9.

To control the actuator for the first task we employ a standard output tracker on the deflection of the spring updating at 1 kHz. The reference function is defined as:

$$y_D = \frac{\tau_A \sin(\omega t)}{k} \tag{4.16}$$

where y_D is the desired output deflection and τ_A is the desired sinusoidal torque

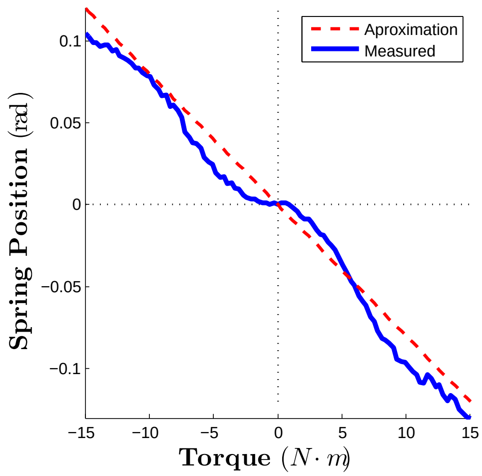

(a) Soft spring: approximated spring constant $k = 125$

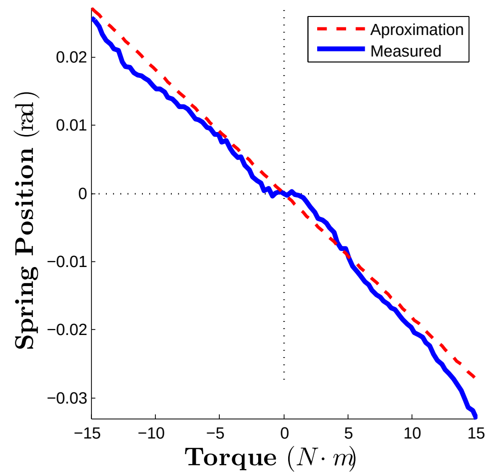

(b) Medium spring: approximated spring constant $k = 550$

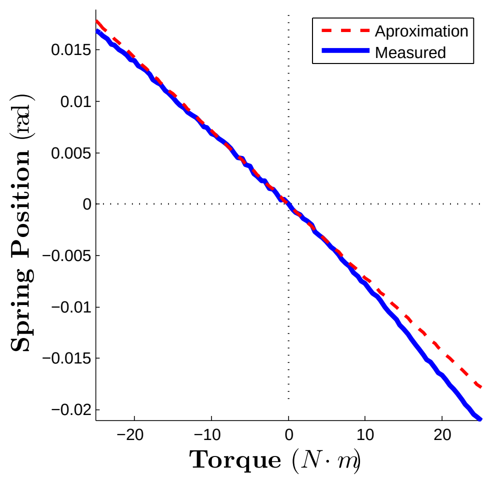

(c) Stiff spring: approximated spring constant $k = 1400$

Figure 4.8: For each spring the motor was commanded to produce a series of open-loop torques. For each torque the corresponding spring deflection was measured. These torque vs. displacement measurements and the approximated functions are plotted above.

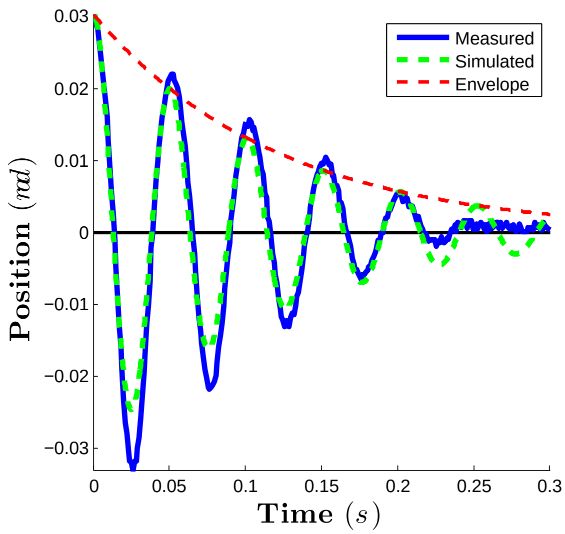

Figure 4.9: To determine the complete dynamic properties of the actuator, we compressed the spring as far as the motor torque limits allowed then cut the power allowing the spring to oscillate the system until friction finally stopped the system. We then fit a simple spring-mass-damper system to the measured response using the spring constant found in Figs. 4.8. Above is an example of the simulated system plotted onto the measured response.

amplitude. We then model the system as a simple spring-mass-damper oscillator in state-space form:

$$\dot{\bar{x}} = A\bar{x} + B\bar{u} \tag{4.17}$$

$$\bar{y} = C\bar{x} \tag{4.18}$$

with the states

$$\bar{x} = \begin{Bmatrix} \theta \\ \dot{\theta} \end{Bmatrix}$$

$$
\text{Soft Spring} \quad \begin{cases} k & 125\ \frac{N\cdot m}{rad} \\ \beta & 1\ \frac{kg\cdot m^2}{s\cdot rad} \\ I_m & 0.055\ kg\cdot m^2 \end{cases}
$$

$$
\text{Medium Spring} \quad \begin{cases} k & 550\ \frac{N\cdot m}{rad} \\ \beta & 1.2\ \frac{kg\cdot m^2}{s\cdot rad} \\ I_m & 0.08\ kg\cdot m^2 \end{cases}
$$

$$
\text{Stiff Spring} \quad \begin{cases} k & 1400\ \frac{N\cdot m}{rad} \\ \beta & 1.5\ \frac{kg\cdot m^2}{s\cdot rad} \\ I_m & 0.09\ kg\cdot m^2 \end{cases}
$$

Table 4.2: The approximated system parameters determined for each fiberglass plate-spring.

where θ is the spring displacement (in radians) and

$$
A = \begin{bmatrix} 0 & 1 \\ \frac{-k}{I} & \frac{-\beta}{I} \end{bmatrix} \tag{4.19}
$$

$$
B = \begin{bmatrix} 0 \\ \frac{1}{I} \end{bmatrix} \tag{4.20}
$$

$$
C = \begin{bmatrix} 1 & 0 \\ 0 & 1 \end{bmatrix}. \tag{4.21}
$$

With the model we can write the model-based output tracking controller as:

$$\begin{aligned} \bar{e} &= \begin{bmatrix} y_D \\ \dot{y_D} \end{bmatrix} - C\bar{x} \\ u &= -K\bar{x} + (CB)^{-1}\left(\ddot{y}_D - C\left(A - BK\right)\bar{x} + K_e\bar{e}\right) \end{aligned} \tag{4.22}$$

where K is is the gain matrix to stabilize the system and K_e are the gains defining the error response.

For the second task we use a standard proportional-derivative controller on the spring compression with a feed-forward torque from the acceleration of the load to try and maintain zero force.

$$\tau_m = K_P k\left(\theta_m - \theta_L\right) + K_D\beta\left(\dot{\theta}_m - \dot{\theta}_L\right) + K_F I_m \ddot{\theta}_L \tag{4.23}$$

4.8 Results - Changing torque against a static surface

For the first task, our controller attempts to apply a sinusoidal torque to a fixed load as in Fig. 4.2. We demonstrate how k, β and I_m affect the maximum frequency

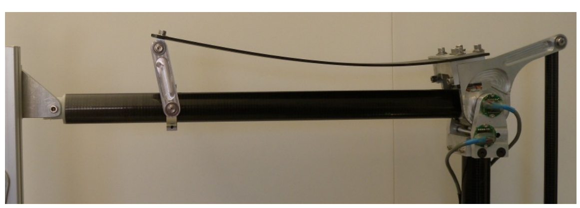

Figure 4.10: For the first task the output of the actuator is clamped to a fixed location. The controller attempts to produce the desired load torque by tracking a sinusoidal displacement between the transmission and output link.

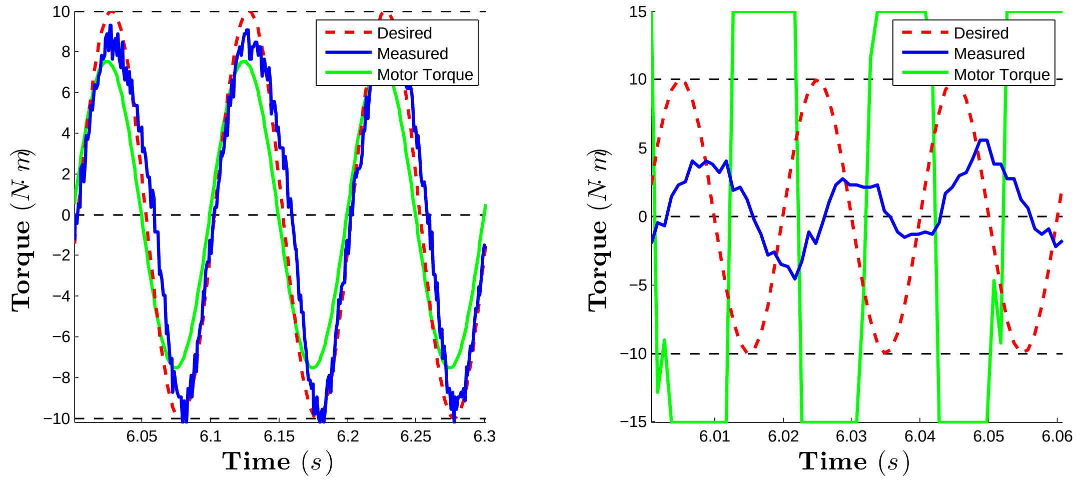

(a) Output tracking example at low frequencies. Because the commanded frequency is low, the motor only has to produce a torque similar to the commanded signal.

(b) Output tracking example at frequencies where the torque required exceeds the limit ($\tau_{limit} = \pm 15\, N \cdot m$ in this case).

Figure 4.11: Output tracking example. The system is trying to produce a sinusoidal torque at the load with an amplitude of $10\, N \cdot m$ around zero with a desired frequency. In Fig. 4.11a the commanded frequency is low so the motor only has to produce a torque similar to the commanded signal. The frequency commanded in Fig. 4.11b requires a torque beyond the capabilities of the motor, causing the output torque to significantly deviate from the desired.

at which the actuator can vary the applied torque experimentally by showing the system performance using three different plate springs. Again, the performance for this task is defined as the frequency that the actuator can oscillate the torque at the load before steady-state error is encountered. As shown in section 4.5, we use the point where the motor torque is saturated to predict this maximum frequency.

For this task, the actuator end-effector is bolted rigidly to the ground with the motor free to compress the spring. Figure 4.10 shows and example of the softest spring under compression. During each test, all angle information is recorded at

1 kHz and by using the spring constants found in section 4.7 we can determine a good estimation of the torques applied to the output.

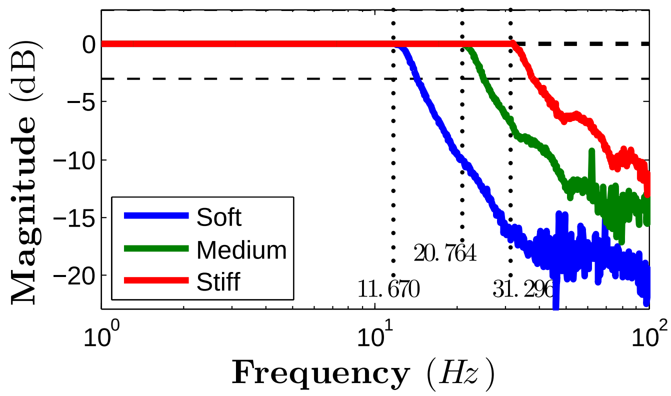

(a) Bode plots of the simulated systems using the parameters in Table 4.2.

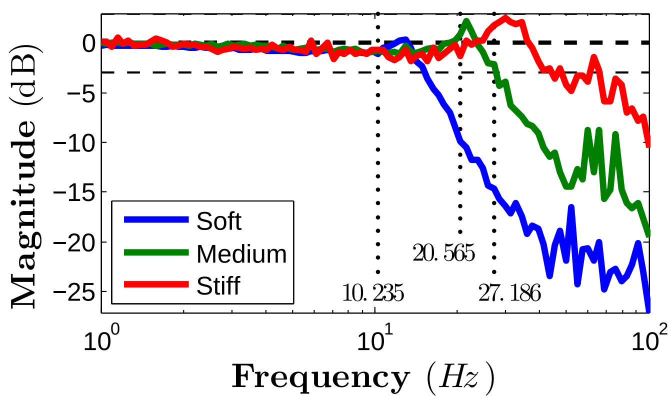

(b) Bode plots of the actual system.

Figure 4.12: Bode plots of the simulated and actual systems applying a steady-state sinusoidal torque with an amplitude of 10 $N \cdot m$ to the output. For each the vertical lines indicate where the commanded motor torque saturated with $\tau_{limit} = \pm 15\ N \cdot m$ at steady-state. Notice how these peak frequencies increase as the system becomes stiffer. For reference, the horizontal dashed line indicates$-3\ dB$.

For each spring we use the controller described in section 4.7 to produce a sinusoidal output torque with an amplitude (τ_A) of 10 $N \cdot m$. An example of how the

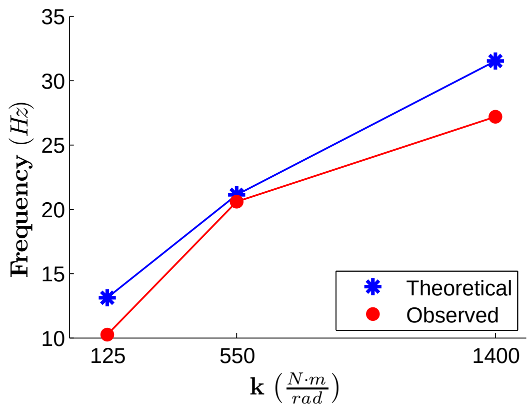

Figure 4.13: These theoretical maximums align very closely to the measured values.

actual system behaves, with $\tau_{limit} = \pm 15\ N \cdot m$, is demonstrated in Fig. 4.11a and 4.11b.

We then step the controller through a range of frequencies between 1 Hz and 100 Hz sampling the spring deflection over a few cycles once the controller has reached steady-state. The measured amplitudes are then converted to decibels and plotted in Fig. 4.12b. To verify the that our controlled system is behaving correctly, we ran the simulated systems using the same controllers over the same frequency ranges to produce the Bode plots in Fig. 4.12a. For each Bode plot we draw a vertical line indicating the frequency (f_{max}) where the commanded motor torque saturates at the torque limit of $\pm 15\ N \cdot m$. As described in section 4.5, the performance of the actuator begins to degrade at this f_{max}.

Using the equation (4.9) in section 4.5 we can find the theoretical frequency that causes τ_m to meet τ_{limit} for the set of parameters (outlined in table 4.2) associated with each plate-spring, and compare it to the observed results.

These theoretical maximums align very closely to the measured values shown in Fig. 4.12b. This implies that the theoretical limits are a good estimation of the maximum performance for an actuator applying a changing torque to a stationary object. Clearly, stiffer impedances increase the maximum performance.

4.9 Results - Zero torque against a moving load

For the second task, our controller attempts to apply a constant zero torque to a sinusoidally reciprocating load as described in section 4.6. We experimentally demonstrate how changing the system's impedance affects the maximum frequency at which the load position can vary before the actuator can no longer maintain the output torque within the desired error bounds.

For this task, the output of the actuator is affixed to a reciprocating mechanism to produce a forced sinusoidal angular displacement. Fig. 4.14 shows an example of the actuator configured with the softest spring. During each test, all angle information

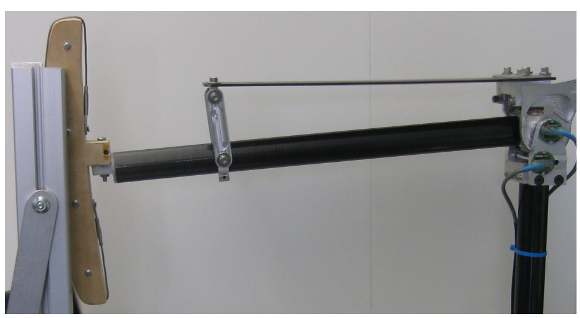

Figure 4.14: For the second task the output of the actuator is affixed to a reciprocating mechanism to produce a forced sinusoidal angular displacement. The controller attempts to produce the desired load torque - a constant zero torque in this case - by tracking the displacement between the transmission and output link.

is recorded at 1 kHz. By using the system constants described in section 4.7 we can determine a good estimation of the torques applied to the output.

For each spring we use the controller outlined in section 4.7 to attempt to produce the desired load torque - a constant zero torque in this case - by tracking the displacement between the transmission and output link. The load motion amplitude is constant between experiments at 0.125 radians. The motor torque limit is set at $\pm 15\ N \cdot m$ with an acceptable torque error at the load of $\pm 5\ N \cdot m$.

We then step the load motion through a range of frequencies, sampling the system state over a few cycles once the actuator has reached steady-state. For each frequency we empirically tune the gains on the controller to maximize the performance.

Using the equation for the load torque using the clipped input as outlined in section 4.6 we can find the theoretical frequency that causes the error in the desired τ_L to reach the chosen tolerances. For the set of parameters (outlined in table 4.2) associated with each plate-spring the theoretical frequencies are compared against

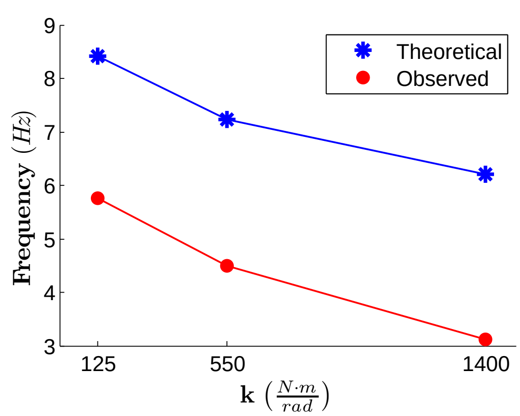

Figure 4.15: Although the observed maximums deviate from the theoretical values, the rate of decrease in performance is similar.

the measured in Fig. 4.15.

Although the observed maximums deviate from the theoretical values, the rate of decrease in performance is similar. It is also reasonable that a real system using an imperfect controller exhibit worse performance than that of the analytically optimal. The discrepancy is likely caused by poor load acceleration estimation, causing error in the feed-forward term of the controller.

These results confirm that that softer impedances increase the maximum performance of an actuator to maintain zero torque against a moving load. It is interesting to note that the performance increase is small even with a fairly large change in spring stiffness.

4.10 Conclusions

In this paper, we have identified the two fundamental tasks an actuator must perform under constant-contact physical interaction: changing forces against a stationary load (position control), and constant forces against a moving load (force control). We analytically show what people have only intuitively known: stiffer systems perform better in position control tasks and softer systems perform better in force control tasks. We demonstrate that there are physical limits - regardless of control strategy - that define the performance of actuators engaged in constant-contact physical interaction tasks. We also show how each component of the actuator contributes to the actuator's performance, and demonstrated the viability of the approach by calculating performance limits for our bench top actuator.

The results of this paper show conclusively that robot actuators that are expected to accomplish both force control and position control tasks must have variable impedance. Force control and position control require exact opposite passive dynamic properties, and share no set of parameters that provide good performance for both tasks. The only way to improve the bandwidth of both tasks simultaneously is to reduce the motor inertia or increase the torque limit, but all motors have torque limits and inertia. Therefore, actuators designed to perform a wide set of tasks require variable impedance. Based on this knowledge, and the methods for calculating bandwidth performance, this paper should provide strong insight into how roboticists should size passive components to achieve their goals.

4.11 Discussion and future work

We derived the physical limitations of actuators with passive dynamics that can be described by the dynamic model shown in Fig. 4.1. Our model does not include active control; we computed the optimal input to the system to produce the required torque at the load with zero or acceptable error. As a result, our results only reflect the physical system's capabilities, and are not dependent on a specific software control strategy. These exact solutions provide the basis for understanding how the parameters affect bandwidth and how to select parameters for a torque control task. Each of these tasks are designed to represent extreme applications of torque and force control under continuous contact. Nonlinearities may affect the system in ways that our models do not predict - although our methods can be used to calculate conservative estimates.

Future work includes the development of relationships for more complex actuation scenarios such as stopping an inertia or mass with initial velocity (catching an object), producing the largest exit velocity within a finite distance (throwing an object), or commanding the actuator to behave like a spring. Real examples of these tasks are spacecraft docking, hammering in a nail, and legged locomotion. This work will inform engineers and robot designers on the roles of elasticity and damping, and provide insight into how each parameter contributes to complex motions.

Chapter 5 – Conclusion

We have derived the physical performance limitations of actuators with passive dynamics that can be described by the dynamic model shown in Fig. 1.1. We computed the optimal input to the system to produce the required torque at the load with zero or acceptable error. This is important so that our results only reflect the physical system's performance. These solutions provide the basis for understanding how the parameters affect bandwidth and how to select parameters for a torque control task. Each of these tasks are designed to represent extreme applications of torque and force control.

In 2 and 4 we have identified the two fundamental tasks an actuator must perform under constant-contact physical interaction: changing forces against a stationary load (position control), and constant forces against a moving load (force control). We analytically show what people have only intuitively known: stiffer systems perform better in position control tasks and softer systems perform better in force control tasks. We demonstrate that there are physical limits - regardless of control strategy - that define the performance of actuators engaged in constant-contact physical interaction tasks. We also show how each component of the actuator contributes to the actuator's performance, and demonstrated the viability of the approach by calculating performance limits for our bench top actuator.

For the model to generate a varying torque against a fixed load, the system should have higher stiffness and/or lower inertia. Perhaps less obvious is that both damping and inertia play a much larger role in increasing the maximum frequency than stiffness.

For the actuator to produce exactly zero torque against a moving load, the system's stiffness does not matter. Instead, the stiffness only determines how quickly the error increases with increased frequency. We found that reducing stiffness decreases error caused by motor torque limits. But as the stiffness approaches infinity, the performance of the actuator is governed solely by the motor inertia and torque limit.

In 3 we identify and describe the fundamental performance of an actuator when experiencing an unexpected impact. We investigated the specific case of catching/stopping an unknown object without allowing it to bounce. We then described the mathematically optimal passive dynamics required to achieve the best possible response, based on fundamental physical limits.

It is shown that by decreasing the stiffness or damping, the maximum velocity that can be caught quickly increases. An interesting note is that the effect of damping on softer springs is much more significant than for stiffer springs. Adding damping has decreasing effect on the maximum displacement of the spring.

There are distinct trade-offs between catching a load with the maximum possible initial velocity and the distances the actuator or spring must travel. To optimize the initial velocity, the designer must decrease the stiffness and damping. However, as the dynamics become softer, the distance that the spring must deflect or that the motor must displace become proportionally larger. This compromise is an important consideration when designing a real physical system.

The general conclusions of this work are summarized as follows:

- **Changing torque against a static surface**
  - Increasing stiffness provides higher bandwidth for applying varying torques to a fixed load.
- **Zero torque against a moving load**
  - Decreasing stiffness provides higher bandwidth for tracking the load motion.
  - Performance increase is small even with a fairly large change in spring stiffness.
- **Catching a mass without bouncing**
  - Decreasing the stiffness quickly increases the maximum velocity that can be caught.
  - As the dynamics become softer, the distance that the spring must deflect or that the motor must displace become proportionally larger. This sets a boundary on how soft a physical system can be before reaching hard limits.

The results of this work show conclusively that robot actuators that are expected to accomplish both force control and position control tasks must have variable impedance. Force control and position control require exact opposite passive dynamic properties, and share no set of parameters that provide good performance for both tasks. The only way to improve the bandwidth of both tasks simultaneously is to reduce the motor inertia or increase the torque limit, but all motors have torque limits and inertia. Therefore, actuators designed to perform a wide set of tasks require variable impedance. Based on this knowledge, and the methods for calculating bandwidth performance, this work should provide strong insight into how roboticists should size passive components to achieve their goals.

Bibliography

[1] G. A. Pratt and M. M. Williamson, "Series elastic actuators," in *IEEE International Conference on Intelligent Robots and Systems*, vol. 1, pp. 399–406, 1995.

[2] D. W. Robinson, *Design and Analysis of Series Elasticity in Closed-Loop Actuator Force Control*. PhD thesis, Massachusetts Institute of Technology, June 2000.

[3] R. M. Alexander, "Three uses for springs in legged locomotion," *The International Journal of Robotics Research*, vol. 9, pp. 53–61, April 1990.

[4] G. A. Cavagna, "Elastic bounce of the body," *Journal of Applied Physiology*, vol. 29, no. 3, pp. 279–282, 1970.

[5] R. J. Full and C. T. Farley, "Musculoskeletal dynamics in rhythmic systems - a comparative approach to legged locomotion," in *Biomechanics and Neural Control of Posture and Movement* (J. M. Winters and P. E. Crago, eds.), New York: Springer-Verlag, 2000.

[6] T. A. McMahon, "The role of compliance in mammalian running gaits," *Journal of Experimental Biology*, vol. 115, pp. 263–282, 1985.

[7] J. W. Hurst and A. A. Rizzis, "Series compliance for an efficient running gait," *IEEE Robotics & Automation Magazine*, vol. 15, pp. 42–51, September 2008.

[8] M. Raibert, *Legged Robots That Balance*. Cambridge, Mass.: MIT Press, 1986.

[9] D. E. Whitney, "Force feedback control of manipulator fine motions," *Journal of Dynamic Systems, Measurement, and Control*, vol. 99, no. 2, pp. 91–97, 1977.

[10] J. D. Schutter, "A study of active compliant motion control methods for rigid manipulators based on a generic control scheme," in *IEEE International Conference on Robotics and Automation*, pp. 1060–1065, 1987.

[11] G. Wyeth, "Demonstrating the safety and performance of a velocity sourced series elastic actuator," in *Robotics and Automation, 2008. ICRA 2008. IEEE International Conference on*, pp. 3642 –3647, May 2008.

[12] J. W. Sensinger and R. F. ff. Weir, "Improvements to series elastic actuators," in *Mechatronic and Embedded Systems and Applications, Proceedings of the 2nd IEEE/ASME International Conference on*, pp. 1 –7, aug. 2006.

[13] N. Tsagarakis, M. Laffranchi, B. Vanderborght, and D. Caldwell, "A compact soft actuator unit for small scale human friendly robots," in *Robotics and Automation, 2009. ICRA '09. IEEE International Conference on*, pp. 4356 –4362, May 2009.

[14] J. Sensinger and R. Weir, "Design and analysis of a non-backdrivable series elastic actuator," in *Rehabilitation Robotics, 2005. ICORR 2005. 9th International Conference on*, pp. 390 – 393, june-1 july 2005.

[15] C.-M. Chew, G.-S. Hong, and W. Zhou, "Series damper actuator: a novel force/torque control actuator," in *Humanoid Robots, 2004 4th IEEE/RAS International Conference on*, vol. 2, pp. 533 – 546 Vol. 2, nov. 2004.

[16] J. Hurst, D. Hobbelen, and A. Rizzi, "Series elastic actuation: Potential and pitfalls," in *International Conference on Climbing and Walking Robots*, 2004.

[17] K. Kemper, D. Koepl, and J. Hurst, "Optimal passive dynamics for torque/force control," in *Robotics and Automation (ICRA), 2010 IEEE International Conference on*, pp. 2149 –2154, May 2010.

[18] J. W. Hurst, J. E. Chestnutt, and A. A. Rizzi, "Series compliance for an efficient running gait: Lessons learned from the ecd leg," *IEEE Robotics and Automation Magazine*, vol. September, pp. 42–51, 2008.

[19] A. Edsinger-Gonzales and J. Weber, "Domo: a force sensing humanoid robot for manipulation research," in *Humanoid Robots, 2004 4th IEEE/RAS International Conference on*, vol. 1, pp. 273 – 291 Vol. 1, nov. 2004.

[20] J. W. Hurst, D. Hobbelen, and A. A. Rizzi, "Series elastic actuation: Potential and pitfalls," in *IROS Workshop*, 2005.

[21] C. An and J. Hollerbach, "Dynamic stability issues in force control of manipulators," in *Robotics and Automation. Proceedings. 1987 IEEE International Conference on*, vol. 4, pp. 890 – 896, Mar. 1987.

[22] B. Bauml, T. Wimbock, and G. Hirzinger, "Kinematically optimal catching a flying ball with a hand-arm-system," in *Intelligent Robots and Systems (IROS), 2010 IEEE/RSJ International Conference on*, pp. 2592 –2599, oct. 2010.

[23] S. Haddadin, A. Albu-Schaffer, A. De Luca, and G. Hirzinger, "Collision detection and reaction: A contribution to safe physical human-robot interaction," in *Intelligent Robots and Systems, 2008. IROS 2008. IEEE/RSJ International Conference on*, pp. 3356 –3363, sept. 2008.

[24] B. Vanderborght, R. Van Ham, D. Lefeber, T. G. Sugar, and K. W. Hollander, "Comparison of mechanical design and energy consumption of adaptable, passive-compliant actuators," *The International Journal of Robotics Research*, vol. 28, no. 1, pp. 90–103, 2009.

[25] M. Zinn, O. Khatib, and B. Roth, "A new actuation approach for human friendly robot design," vol. 1, pp. 249 – 254 Vol.1, april-1 may 2004.